Constitutional, Metabolic, and Related Disorders

4

Kristian T. Schafernak and Katherine R. Calvo

This chapter illustrates and describes the bone marrow features of inherited bone marrow failure syndromes (e.g., Fanconi anemia, Diamond-Blackfan anemia, Shwachman-Diamond syndrome, and dyskeratosis congenita), as well as acquired diseases such as aplastic anemia and paroxysmal nocturnal hemoglobinuria, which can have overlapping morphologic features and are often included in the differential diagnosis of young cytopenic patients) (Figs. 4.1, 4.2, 4.3, 4.4, 4.5, 4.6, and 4.7). Increasingly, it is recognized that adolescents and adults may harbor germline mutations in *GATA2* (Fig. 4.8), *RUNX1* (Fig. 4.23), and other genes, which predispose to marrow failure, myelodysplasia, and myeloid malignancy. The bone marrow features of other inherited diseases presenting with cytopenias and impaired immunity are also illustrated, including CTLA4 deficiency (Fig. 4.9), autoimmune lymphoproliferative syndrome (ALPS) (Fig. 4.10), activated PI3K-delta syndrome (Figs. 4.11, 4.12, 4.13, 4.14, 4.15, 4.16, and 4.17), Chédiak-Higashi syndrome (Figs. 4.18, 4.19, and 4.20), WHIM syndrome (Fig. 4.21), and chronic granulomatous disease (Fig. 4.22). Inherited diseases resulting primarily in single-lineage cytopenias involving erythroid (e.g., severe congenital neutropenia (Fig. 4.5)), myeloid (e.g., severe congenital neutropenia (Fig. 4.5)), and platelets (e.g., familial thrombocytopenia (Fig. 4.23)) are also presented. Marrow diseases associated with toxic and/or metabolic states and storage diseases (e.g., Gaucher disease (Fig. 4.24), Niemann-Pick disease (Figs. 4.25, 4.26, and 4.27), hemophagocytic lymphohistiocytosis (Fig. 4.28), megaloblastic anemia (Figs. 4.29, 4.30, and 4.31), arsenic toxicity (Fig. 4.32), renal osteodystrophy (Fig. 4.33), and osteopetrosis (Fig. 4.34) are included in this chapter.

K.T. Schafernak
Department of Pathology and Laboratory Medicine, Phoenix Children's Hospital, Phoenix, AZ, USA
e-mail: kschafernak@phoenixchildrens.com

K.R. Calvo, M.D. Ph.D. (✉)
Department of Laboratory Medicine, National Institutes of Health Clinical Center, 10 Center Dr. Bldg 10/2C306 Bethesda, MD 20892-1508, USA
e-mail: calvok@nih.gov

T.I. George, D.A. Arber (eds.), *Atlas of Bone Marrow Pathology*, Atlas of Anatomic Pathology,
https://doi.org/10.1007/978-1-4939-7469-6_4

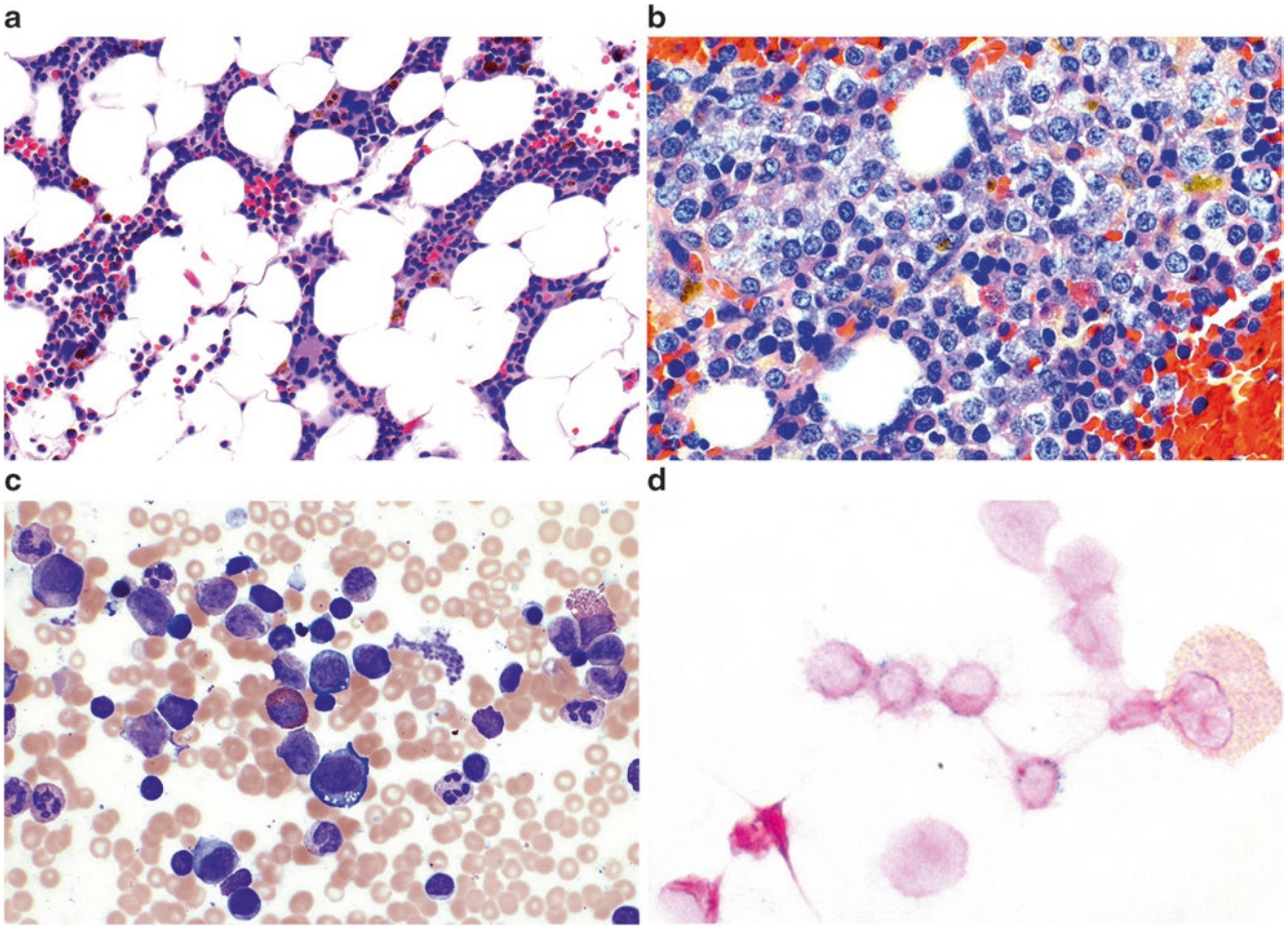

Fig. 4.1 Diamond-Blackfan anemia (DBA). DBA is an inherited bone marrow disorder caused by germline mutations in genes encoding ribosomal proteins (e.g., *RPS19*, *RPL5*). Onset is typically at birth or in early infancy. Initially, the bone marrow in DBA may be normocellular with only profound erythroid hypoplasia. (**a**) This 5-year-old's bone marrow is hypocellular and also has a decreased number of myeloid precursors. (**b**) This particle clot section shows a profound erythroid hypoplasia and increased storage iron as a sequela of blood transfusion. (**c**) Occasionally, the erythroid precursors in DBA contain cytoplasmic vacuoles. Note the full maturation of myeloid precursors and a few hematogones in the background. (**d**) Ring sideroblasts are sometimes seen in DBA, as in this case

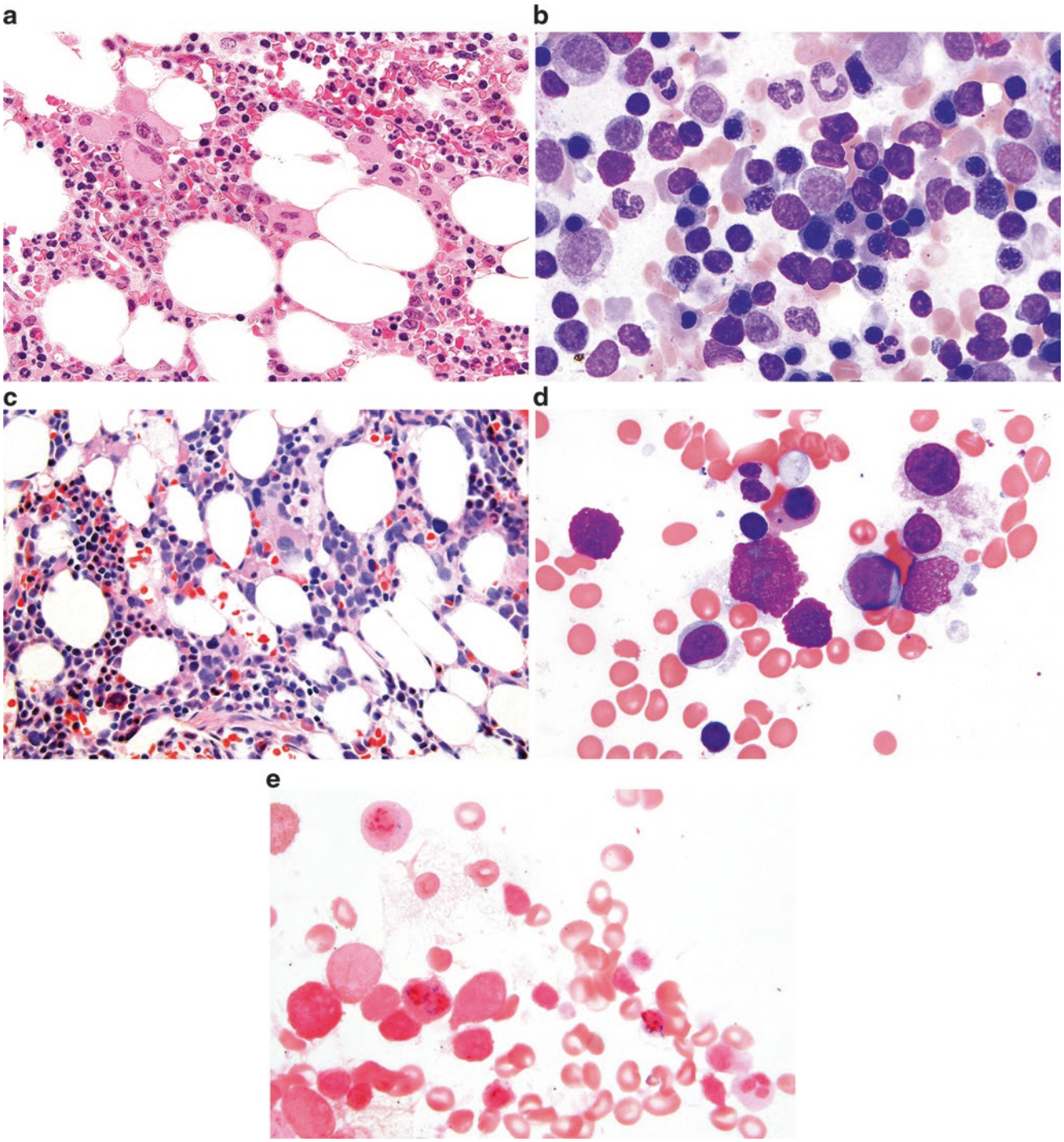

Fig. 4.2 Fanconi anemia. Fanconi anemia is caused by germline mutations in any 1 of currently 20 genes, the most common involving *FANCA*, *FANCC*, and *FANCG*. Patients develop bone marrow failure and have an increased risk of progression to myelodysplastic syndrome (MDS)/acute myeloid leukemia (AML). (**a**) This bone marrow core biopsy is from a 10-year-old boy with Fanconi anemia and pancytopenia. The bone marrow is hypocellular for the patient's age, with focal clustering of hypolobated megakaryocytes. (**b**) The aspirate smear shows a relative erythroid predominance and myeloid hypoplasia without increased blasts. Cytogenetic analysis showed a normal karyotype. About one third of Fanconi anemia patients go on to develop a hematologic malignancy, and some are even diagnosed with MDS or AML on their first bone marrow examination. In a different case, an 8-year-old boy with progressive fatigue was found to be anemic. He was previously healthy, with previous workups only for short stature/failure to thrive. His mother had died from breast cancer 5 years earlier. The bone marrow was hypocellular for age (**c**) and showed trilineage dysplasia with blasts in the 10–15% range (**d**) and numerous ring sideroblasts (**e**). The final diagnosis was MDS, refractory anemia with excess blasts-2 (RAEB-2) with complex cytogenetic abnormalities. A diepoxybutane (DEB) clastogen assay was positive, and genetic testing was also pursued, particularly in light of the family history

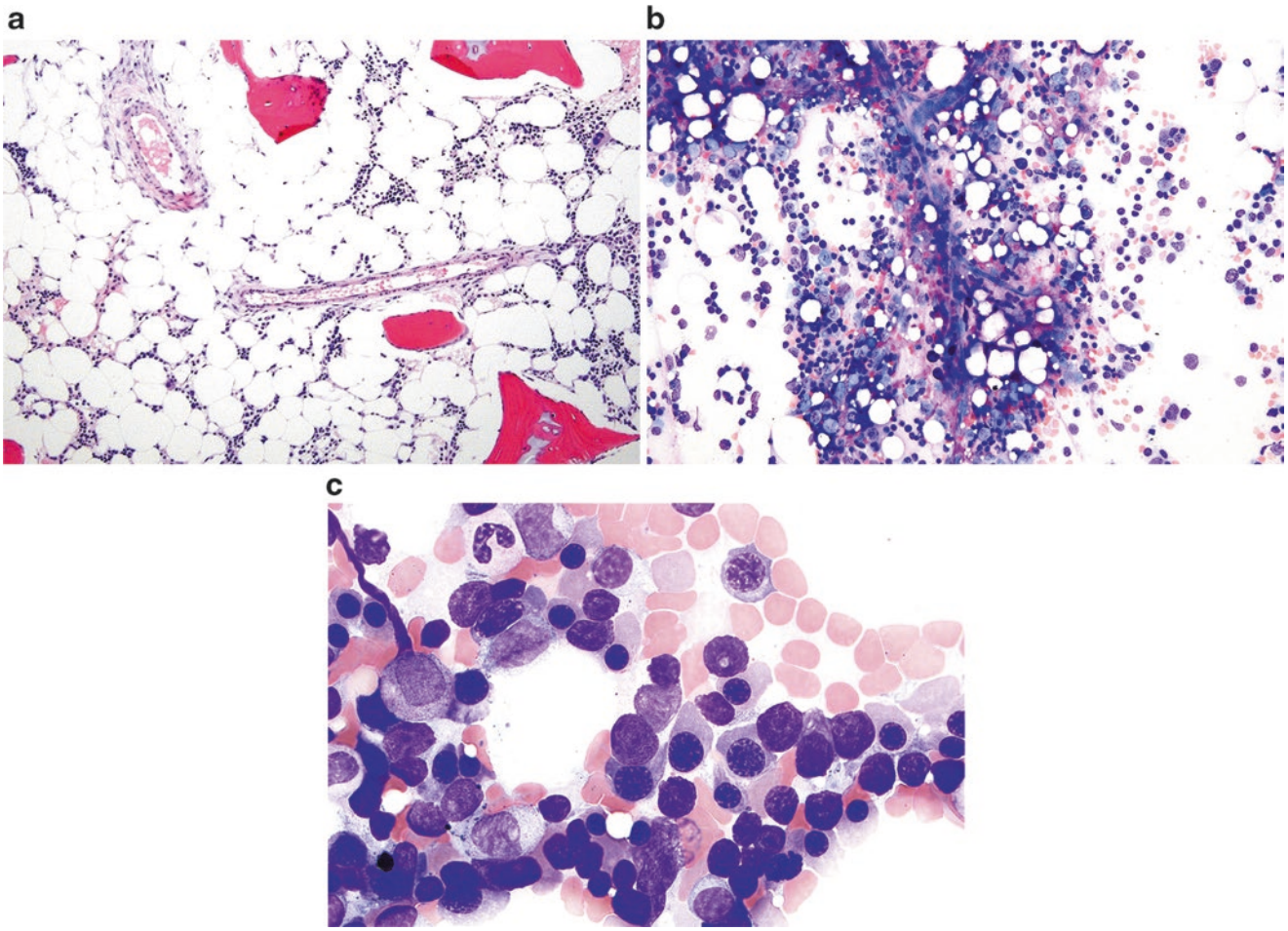

Fig. 4.3 Shwachman-Diamond syndrome (SDS). SDS is associated with germline mutations in the *SBDS* gene. Neutropenia is the most common cytopenia in SDS, although mild anemia and thrombocytopenia may also be present. Bone marrow cellularity is highly variable, ranging from hypoplastic to hypercellular, and does not correlate well with the degree of peripheral cytopenias. Children with SDS often present with bone marrows that are hypocellular for their age (**a**), with diminished multilineage hematopoiesis and relatively hypoplastic and left-shifted granulopoiesis (**b** and **c**). Because mild morphologic dysplasia is commonly seen in SDS, caution should be taken not to overinterpret it as MDS, although these patients are certainly at risk for MDS/AML. Furthermore, cytogenetic analysis in surveillance marrows may be associated with frequent appearance (and disappearance) of clones

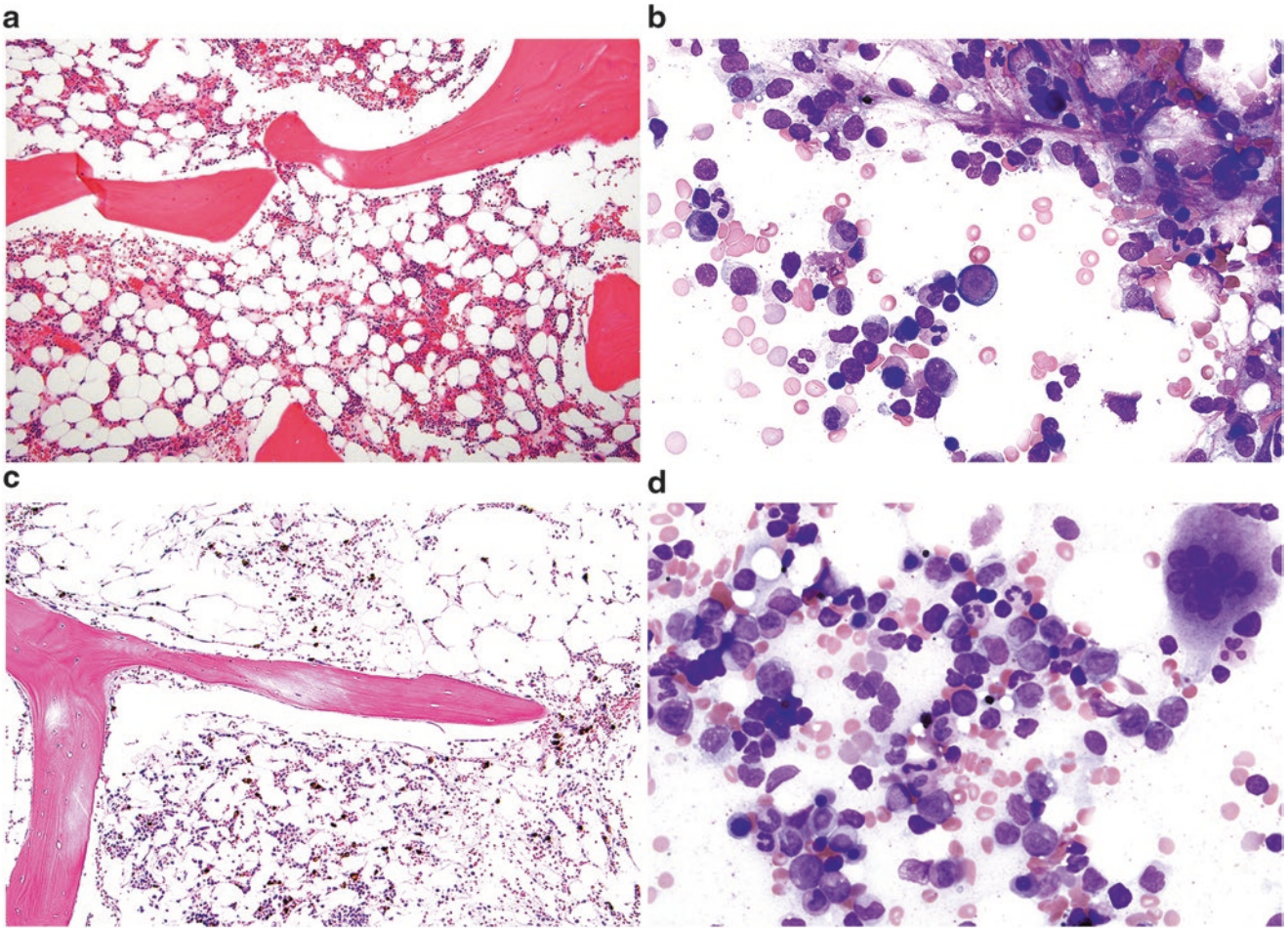

Fig. 4.4 Telomere diseases/dyskeratosis congenita. Dyskeratosis congenita and telomere diseases result from mutations in one of many genes, including *DKC1*, *TERT*, and *TERC*. Telomerase is a ribonucleoprotein complex that synthesizes/elongates telomeres to counteract the attrition that occurs with cell division. *TERT* encodes the telomerase enzyme, whereas *TERC* encodes the RNA template. *DKC1* is present on the X chromosome and encodes dyskerin, another protein associated with the complex, without which it becomes destabilized. Dyskeratosis congenita frequently refers to a bone marrow failure state with a classic triad of dystrophic nails, oral leukoplakia, and lacy, reticular skin pigmentation of the upper chest and neck, sometimes accompanied by mental retardation or other manifestations. Mutations in *TERT* and *TERC* and other genes in the telomere complex cause disease in children and adults characterized by bone marrow failure as well as pulmonary fibrosis, liver disease, and premature graying of hair. (**a**) and (**b**) Macrocytosis and thrombocytopenia were found in a previously healthy 16-year-old boy prior to surgery to repair a femur fracture sustained in a sports accident. Examination revealed that his bone marrow was hypocellular for age (30–35% cellular) with diminished multilineage hematopoiesis and a relative mild megaloblastoid erythroid hyperplasia but no increase in blasts. He was subsequently found to have extremely short telomeres and a heterozygous mutation in *TERT*. (**c**) and (**d**) A hypocellular marrow is present in a 9-year-old girl with a germline heterozygous mutation in *TERT* with moderate pancytopenia. The aspirate smear shows decreased progressive myelopoiesis and erythropoiesis without overt dysplasia. (**e**) Flow cytometry with fluorescence in situ hybridization (Flow-FISH) analysis demonstrates decreased telomere length in lymphocytes and granulocytes (black circle) from a young adult with pancytopenia and germline *TERC* mutation

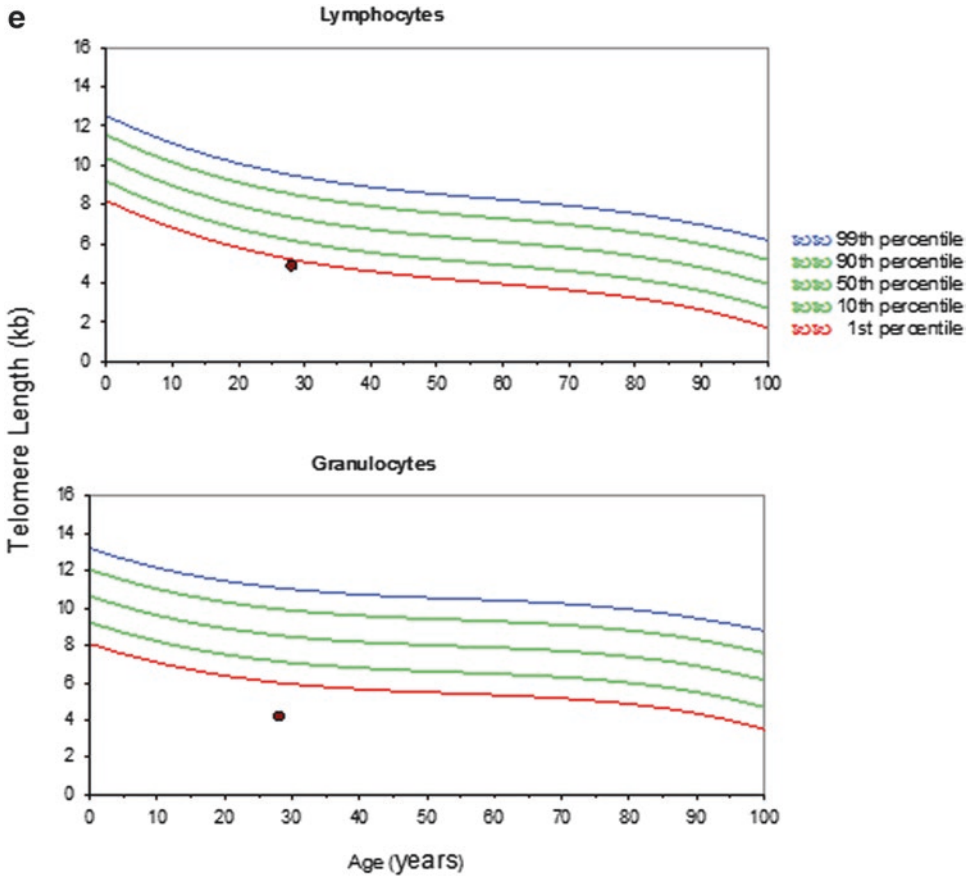

Fig. 4.4 (continued)

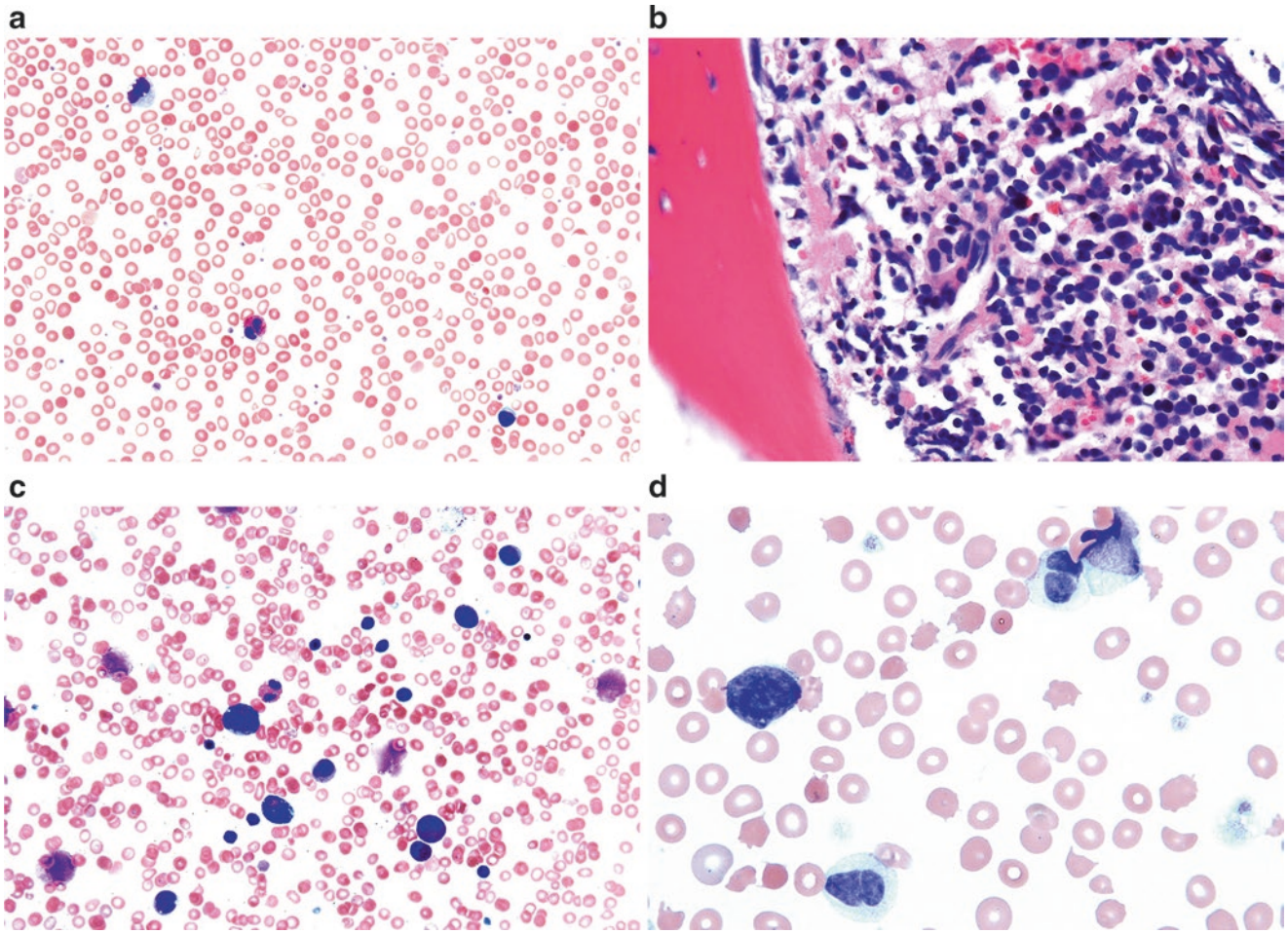

Fig. 4.5 Severe congenital neutropenia (SCN). In a 12-week-old boy, first-degree heart block, dermatitis, and neutropenia were all attributed to neonatal lupus erythematosus, as his mother had been diagnosed earlier with discoid lupus erythematosus. (**a**) No segmented neutrophils could be identified on his peripheral blood smear, although mature eosinophils were present. (**b**) and (**c**) Bone marrow examination revealed a prominent lymphoid component as physiologic hematogone hyperplasia, which typically occurs in the first month of life and persists for the first couple of years. However, a maturation arrest was observed in the neutrophil series; occasional promyelocytes and very rare neutrophilic myelocytes and metamyelocytes were seen without definite band forms or segmented neutrophils. We felt this might represent an alloimmune phenomenon associated with neonatal lupus erythematosus (which would be determined to some extent by a compatible clinical evolution but would tend to be associated with a later "block" in maturation), but we could not exclude severe congenital neutropenia/Kostmann syndrome. A mutation was found in his *ELANE* gene, which is associated with autosomal dominant severe congenital (static) neutropenia, as well as cyclic neutropenia. (**d**) A feared complication of SCN is shown here, with development of MDS/AML in a girl who had been receiving long-term therapy with granulocyte-colony stimulating factor

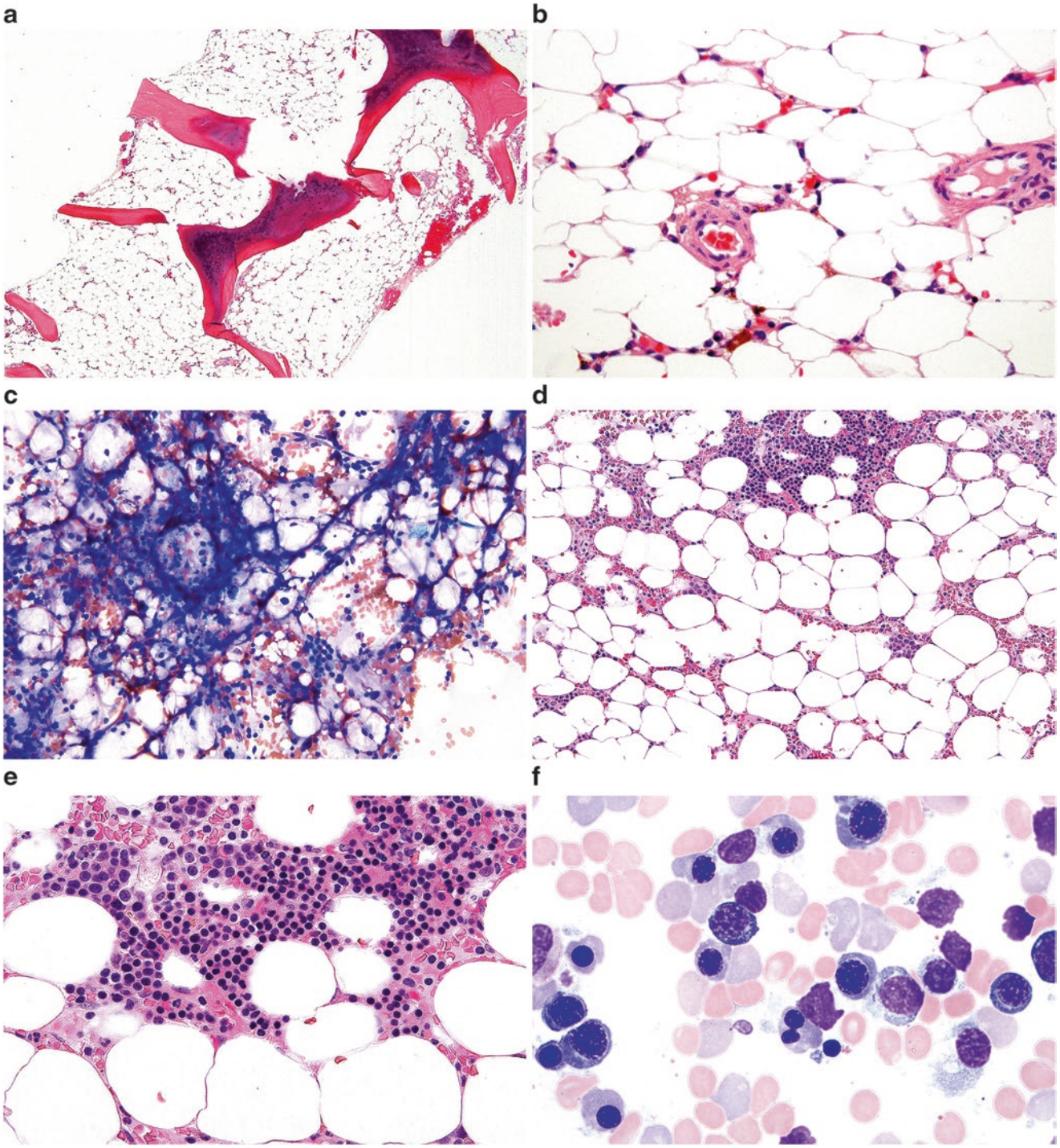

Fig. 4.6 Aplastic anemia (AA) and AA with a paroxysmal nocturnal hemoglobinuria (PNH) clone. Idiopathic AA is largely thought to be an acquired disease with autoimmune etiology, but the features overlap with many inherited bone marrow failure syndromes, and genetic testing may be required to rule out inherited bone marrow failure. Of patients with acquired AA, approximately 10–15% ultimately develop MDS, which suggests a component of underlying primary marrow disease in some patients. Patients with AA frequently harbor somatic mutations in *PIGA*, resulting in PNH clones. (**a**) This low-power image of a trephine biopsy from a teenage girl with AA whose marrow is diffusely and markedly hypocellular for age. (**b**) High-power image of an H&E-stained bone marrow biopsy section shows profound hypocellularity. The few remaining hematopoietic cells are lymphocytes, plasma cells, and macrophages with pigment in their cytoplasm. (**c**) Wright-Giemsa-stained bone marrow aspirate smear contains a profoundly hypocellular particle with prominent stromal elements including fat cells and capillaries lined by endothelial cells and few residual hematopoietic cells (mostly lymphocytes and macrophages). (**d**) Bone marrow from a 23-year-old man with AA and a PNH clone. The PNH clone was detected by flow cytometry analysis of the peripheral blood and involved 99% of neutrophils. (**e**) At higher magnification, note foci of erythropoiesis frequently seen in hypocellular marrows of patients with AA and PNH clones. (**f**) Aspirate smear shows an erythroid predominance and nuclear budding in occasional erythroid precursors from the same patient with AA and PNH. Occasional nuclear budding and binucleation of erythroid precursors (typically involving less than 10% of the erythroid precursors) can be seen in patients with PNH clones. Caution must be used not to overinterpret these changes as evidence of dysplasia in patients with PNH

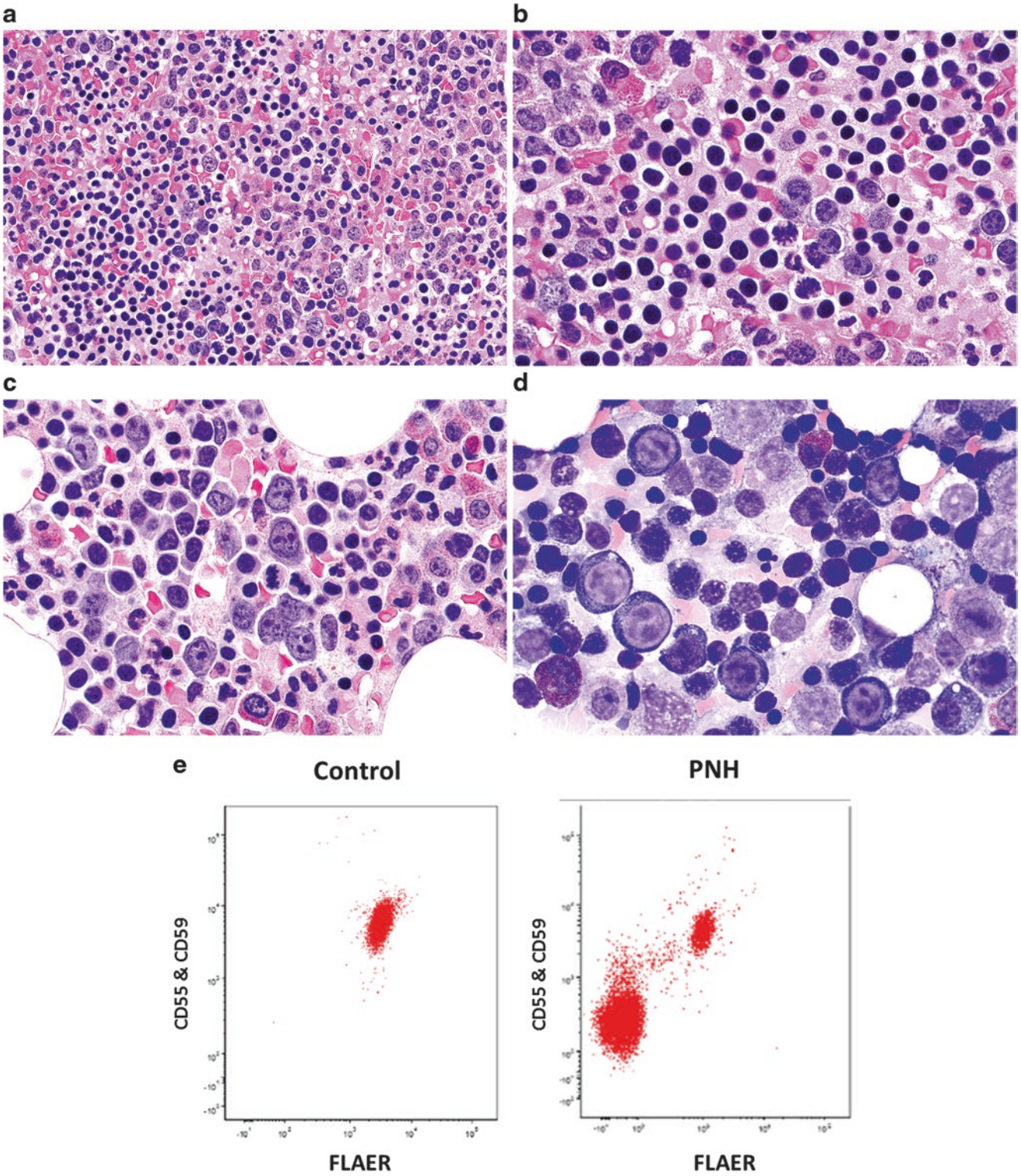

Fig. 4.7 Paroxysmal nocturnal hemoglobinuria. PNH is characterized by acquired somatic mutations in the *PIGA* gene, leading to loss of GPI-linked proteins on red blood cells (RBCs) and white blood cells, and subsequent destruction of RBCs by the complement system. Patients suffer from intravascular hemolysis, with an increased risk of thrombosis. (**a**) and (**b**) This bone marrow core biopsy from a woman with PNH shows a hypercellular marrow with erythroid hyperplasia. (**c**) Frequently, erythropoiesis is left-shifted with large cells with dispersed blast-like chromatin on H&E stain. (**d**) Aspirate smear shows left-shifted erythropoiesis and occasional nuclear budding consistent with stressed erythropoiesis. Flow cytometric analysis has largely replaced earlier tests (sucrose lysis test and Ham's acid hemolysis test) for PNH. (**e**) Peripheral blood neutrophils show normal expression of CD55, CD59, and FLAER in cells from a healthy control (left plot). In contrast, a large population of neutrophils in the patient with PNH has lost expression of CD55, CD59, and FLAER (*right plot*), representing a PNH clone of approximately 75% in this patient

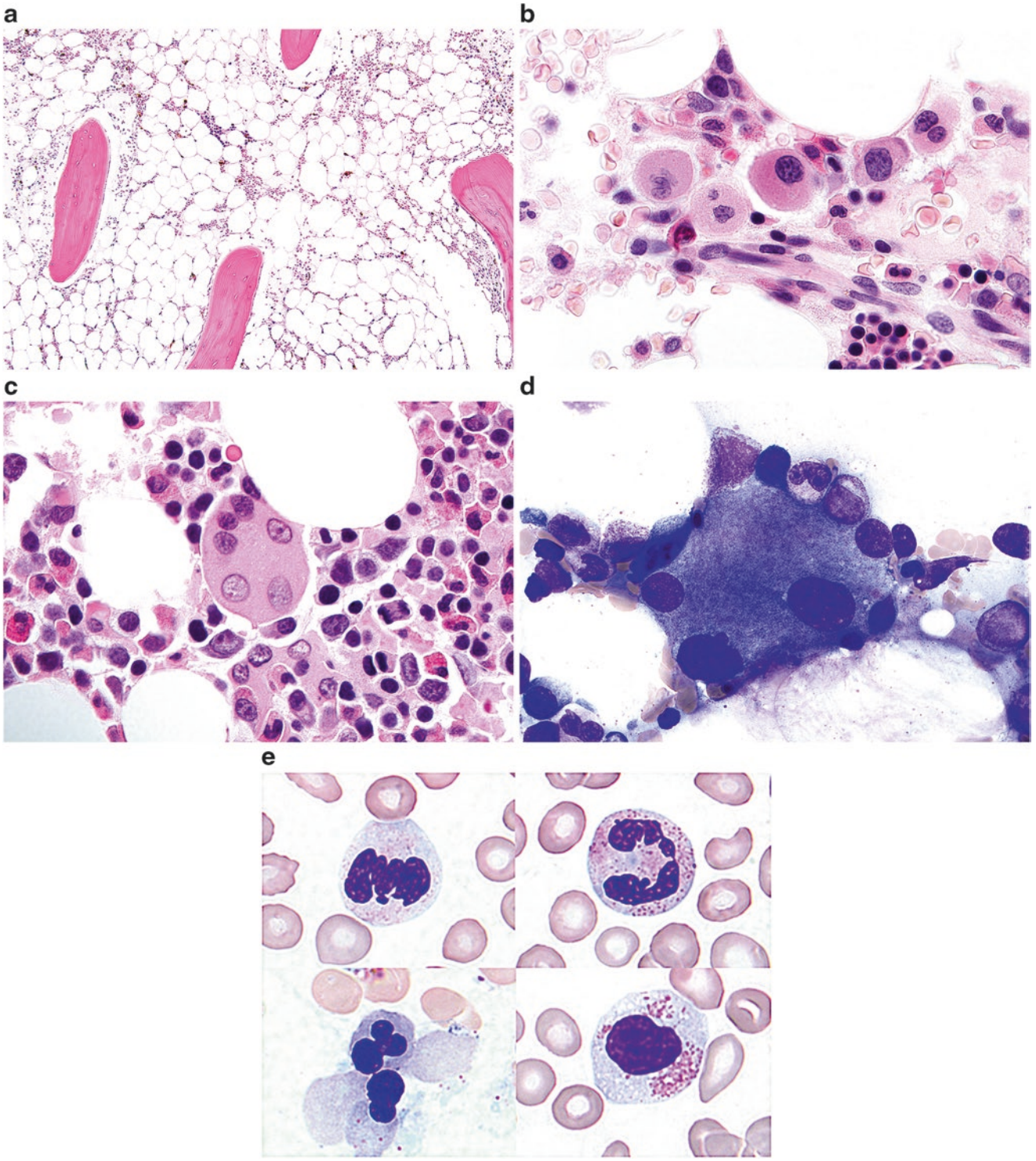

Fig. 4.8 GATA2 deficiency. GATA2 is a transcription factor that is critical for normal hematopoiesis. Germline heterozygous mutations in *GATA2* lead to a spectrum of bone marrow disease that overlaps with aplastic anemia (AA), hypocellular MDS/AML, and chronic myelomonocytic leukemia (CMML). Patients may have a family history of AA, MDS, AML, or CMML. Many patients present with a history of warts and/or severe immunodeficiency characterized by loss of monocytes, B cells, B-cell precursors, NK cells, and dendritic cells, with opportunistic infections such as *Mycobacterium avium* complex. (**a**) Bone marrow biopsy from a 19-year-old man with pancytopenia and a previous diagnosis of AA. The bone marrow is markedly hypocellular for the patient's age. (**b**) Close examination on higher power reveals clusters of atypical, hypolobated megakaryocytes. Cytogenetic analysis of this marrow specimen revealed monosomy 7, and a germline mutation in *GATA2* was identified. The final diagnosis was myelodysplasia with germline *GATA2* mutation. (**c**) and (**d**) Bone marrow from a 36-year-old man with a history of warts and recent cytopenias. Note the characteristic large, osteoclast-like megakaryocytes with multiple separated nuclear lobes on the core biopsy (**c**) and aspirate smear (**d**), which are common in patients with GATA2 deficiency. Cytogenetic analysis showed trisomy 8, and a germline *GATA2* mutation was identified. (**e**) Composite of atypical cells commonly seen in GATA2 deficiency, including hypogranular and/or hyposegmented granulocytes and dyserythropoietic red cell precursors

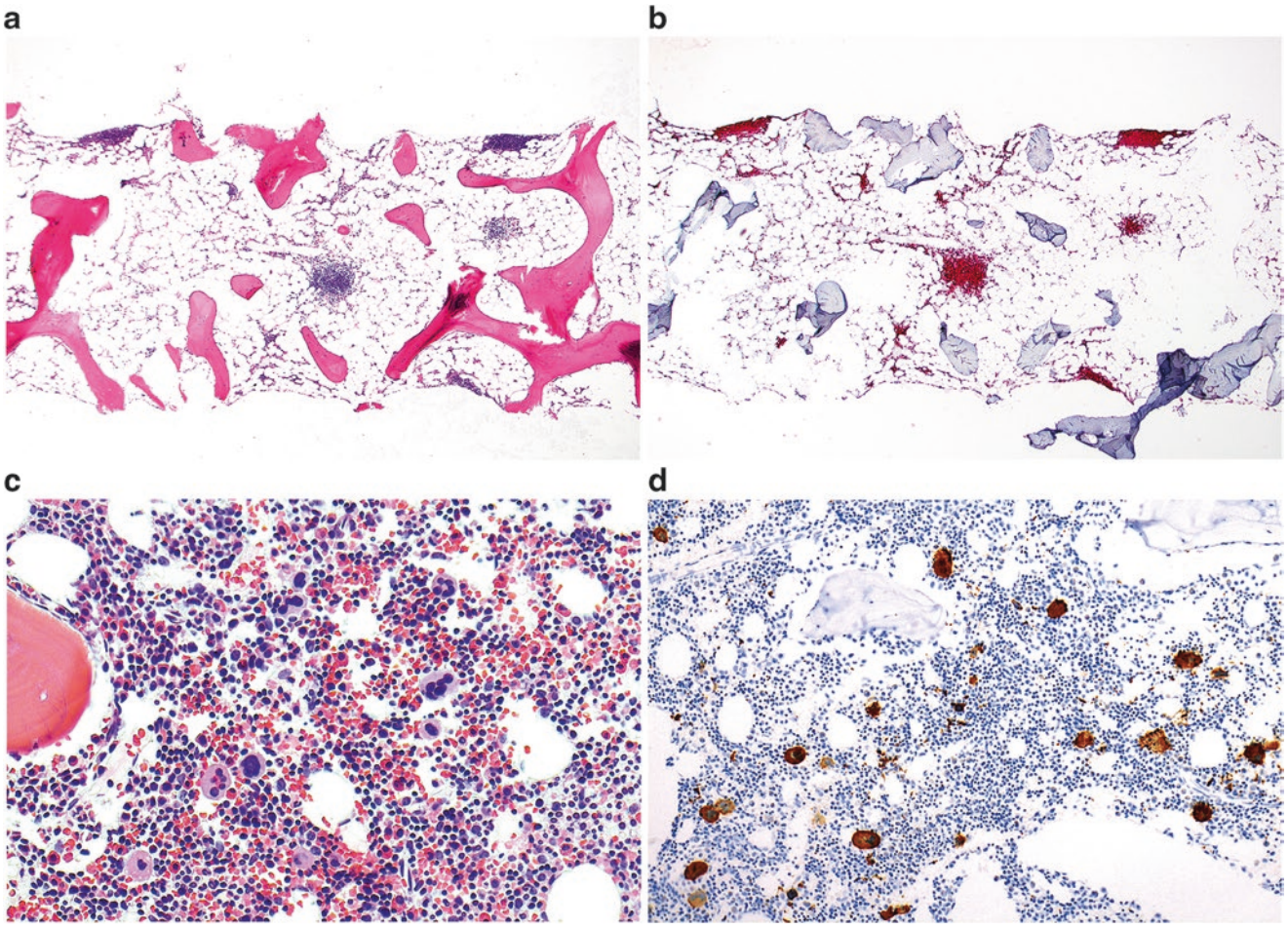

Fig. 4.9 CTLA4 deficiency. Patients with heterozygous germline mutations in the gene encoding cytotoxic T-lymphocyte antigen-4 (*CTLA4)* can present with severe immune dysregulation leading to autoimmune cytopenias, B-cell lymphopenia, and lymphocytic infiltrates in multiple organs. The bone marrow features show a morphologic spectrum overlapping with AA, large granular lymphocytic leukemia (LGL), and immune thrombocytopenic purpura (ITP). (**a**) Bone marrow core biopsy from an 18-year-old woman with pancytopenia. The marrow is markedly hypocellular for the patient's age, with trilineage hypoplasia resembling an aplastic marrow. Additionally, multiple distinct lymphoid aggregates are identified, which are composed of small- to medium-sized lymphocytes. (**b**) Immunohistochemistry (IHC) for CD3 showed that the lymphocytic aggregates were composed of T cells that were predominantly CD4-positive. IHC for CD8 revealed a subtle yet diffuse interstitial CD8-positive T-cell infiltrate (*not shown*). IHC for CD20 showed near absence of B cells (*not shown*). Molecular genetic studies showed an abnormal T-cell gene rearrangement pattern (oligoclonal). Genetic sequencing revealed a germline heterozygous mutation in *CTLA4*. (**c**) and (**d**) An 8-year-old boy initially presented at age 7 with marked thrombocytopenia with a high immature platelet fraction. He responded to two doses of intravenous immune globulin with brief but nonsustained normalization of the platelet count. In addition, there was an absolute neutropenia and mild anemia; the neutropenia resolved, but the anemia was stable. Bone marrow examination showed megakaryocytic hyperplasia (**C**, H&E stain; (**d**), CD61 IHC stain), consistent with the clinical diagnosis of ITP. Subsequently, platelet-specific and neutrophil antibodies were demonstrated; taken together with lymphadenopathy and splenomegaly, these results suggested autoimmune lymphoproliferative syndrome (ALPS). An ALPS panel by flow cytometry revealed 2.3% TCRαβ CD4,CD8 double-negative T cells (0.3–1.7). No mutations were identified in *FAS* (*TNFRSF6*), *FASLG* (*TNFSF6*), or *CASPASE 10*, three of the most common genes implicated in ALPS. Three years later, the patient presented with neurological symptoms and was found to have a large tumorlike inflammatory brain lesion, which led to sequencing and discovery of a heterozygous germline *CTLA4* mutation

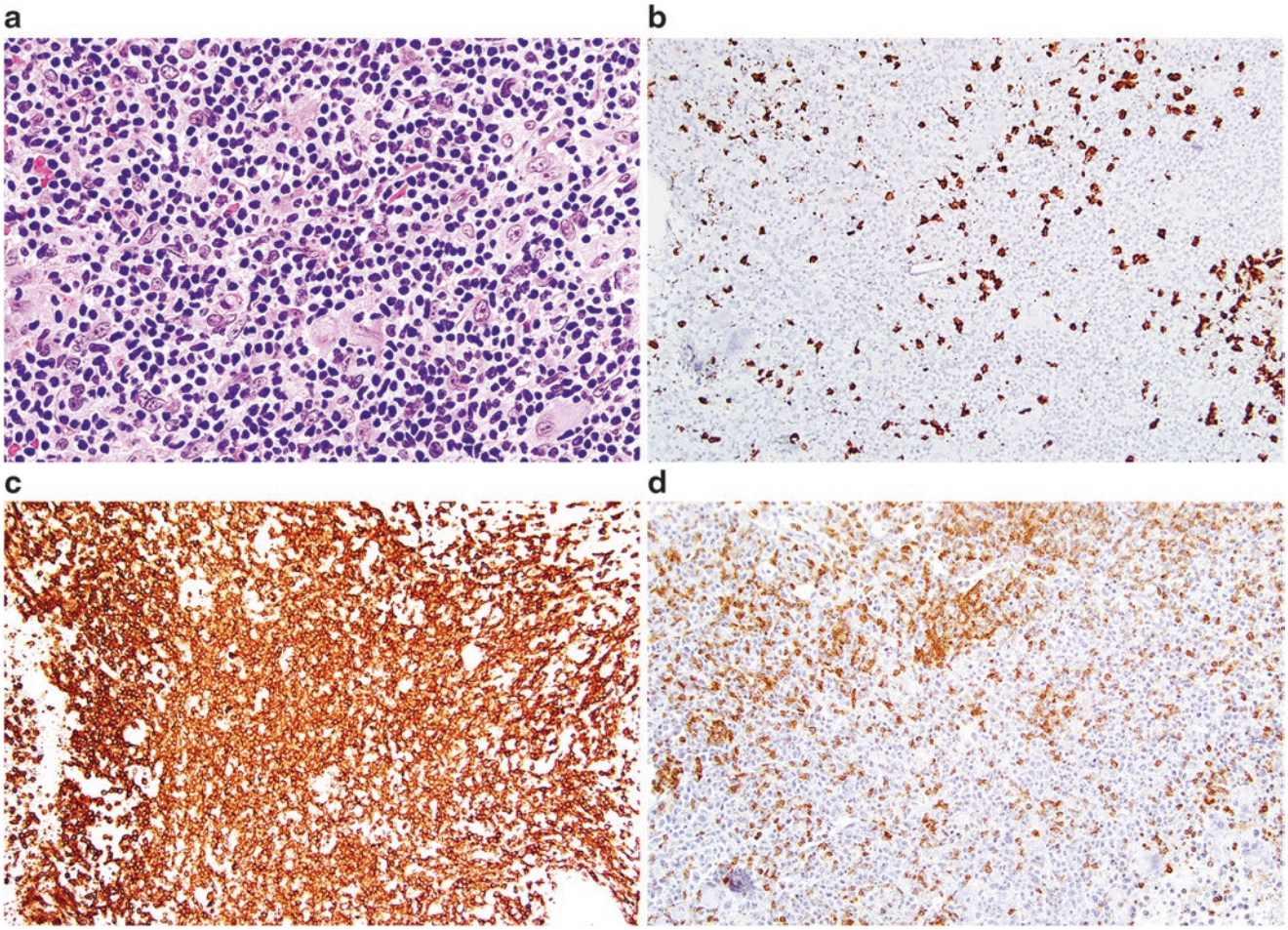

Fig. 4.10 Autoimmune lymphoproliferative syndrome (ALPS). Patients with ALPS have germline mutations in one of several genes critical for FAS-mediated lymphocyte apoptosis, including *FAS*, *FASL*, and *CASP 10*. Patients can present with autoimmune cytopenias, lymphadenopathy, splenomegaly, and hypergammaglobulinemia, and they have an increased risk of developing lymphoma. The hallmark of ALPS is increased numbers of CD4 and CD8 double-negative T cells (DNTs). The bone marrow in patients with ALPS typically shows lymphocytosis with non-paratrabecular lymphoid aggregates (**a**). In this case from a patient with a germline *FAS* mutation, the lymphoid aggregates are primarily composed of T cells highlighted by CD3 immunohistochemistry (IHC) (**c**), with occasional admixed B cells highlighted by CD20 IHC (**b**). CD45RO IHC staining (**d**) is significantly less than CD3, consistent with the presence of increased DNTs (*Courtesy of* Dr. Irina Maric)

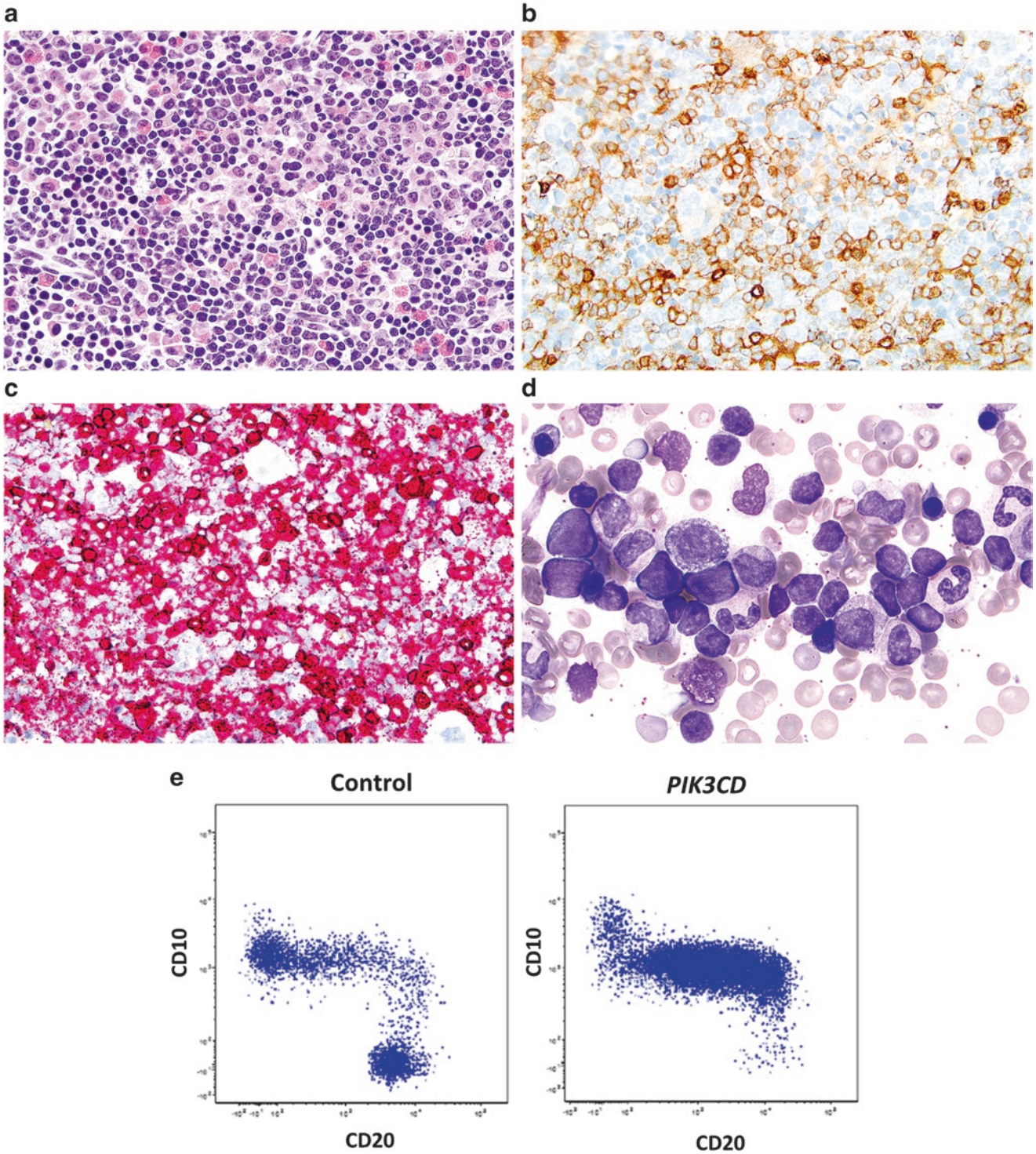

Fig. 4.11 Activated PI3K-delta syndrome. Germline gain-of-function mutations in *PIK3CD* can lead to a syndrome characterized by cytopenias, immunodeficiency, lymphoproliferation in tissues, lymphopenia in the peripheral blood, cytomegalovirus, and Epstein-Barr virus (EBV) viremia, with an increased risk of developing B-cell lymphomas. (**a**) This bone marrow is from a 5-year-old boy with cytopenias and a germline mutation in *PIK3CD*. The marrow is hypercellular, with hematogone or precursor B-cell hyperplasia. Immunohistochemistry for CD10 (**b**) and CD79a (**c**) shows an abundance of B-cell precursors. (**d**) The aspirate smear shows frequent immature lymphoid precursors, many of which have blast-like chromatin. Flow cytometric analysis shows an abnormal B-cell maturation pattern in the CD19+ lymphoid compartment. (**e**) Bone marrow from a healthy pediatric control, for comparison. The B-cell compartment of the patient with activated PI3K-delta syndrome shows an abundance of CD10+ B-cell precursors with a near absence of mature CD10−/CD20+ B cells. This pattern resembles a maturation arrest at the transitional B-cell or late hematogone stage. These findings may overlap with maturation arrest observed in an acute leukemia, so they should be interpreted with caution

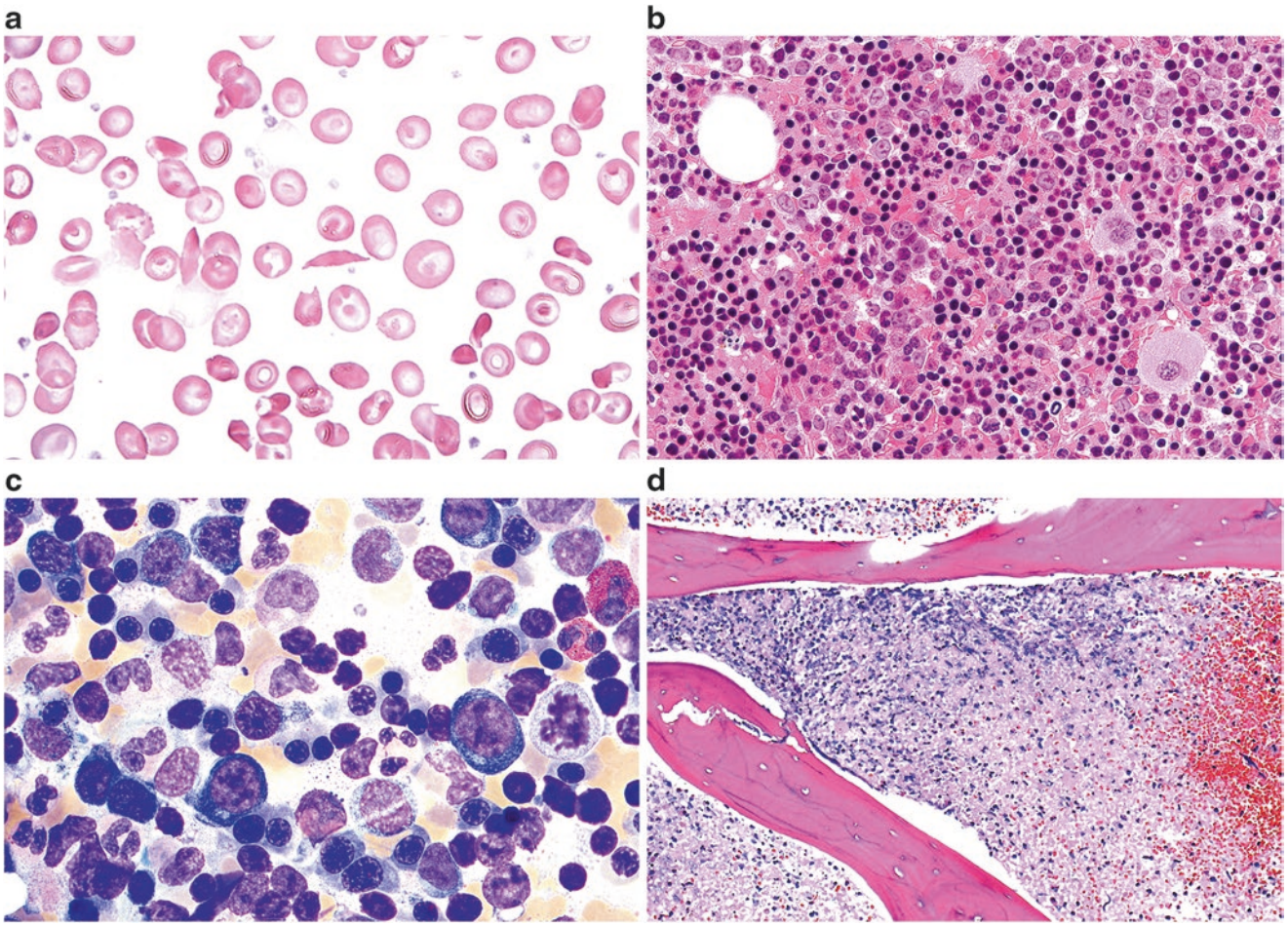

Fig. 4.12 Sickle cell anemia (SCA). SCA is an inherited hemoglobinopathy with RBCs that contain abnormal hemoglobin causing rigid sickling of the RBCs. (**a)** This peripheral smear from a 20-year-old man with hemoglobin SS shows RBCs with marked anisocytosis and poikilocytosis, sickle cells, numerous target cells, Howell-Jolly bodies, and Pappenheimer bodies. The bone marrow core biopsy is hypercellular (**b**). Evidence of erythroid hyperplasia is seen on both the core biopsy and the aspirate smear (**c**), as evidenced by an inverted M:E ratio. The bone marrow biopsy from a separate patient (**d**) shows necrosis and acute inflammation

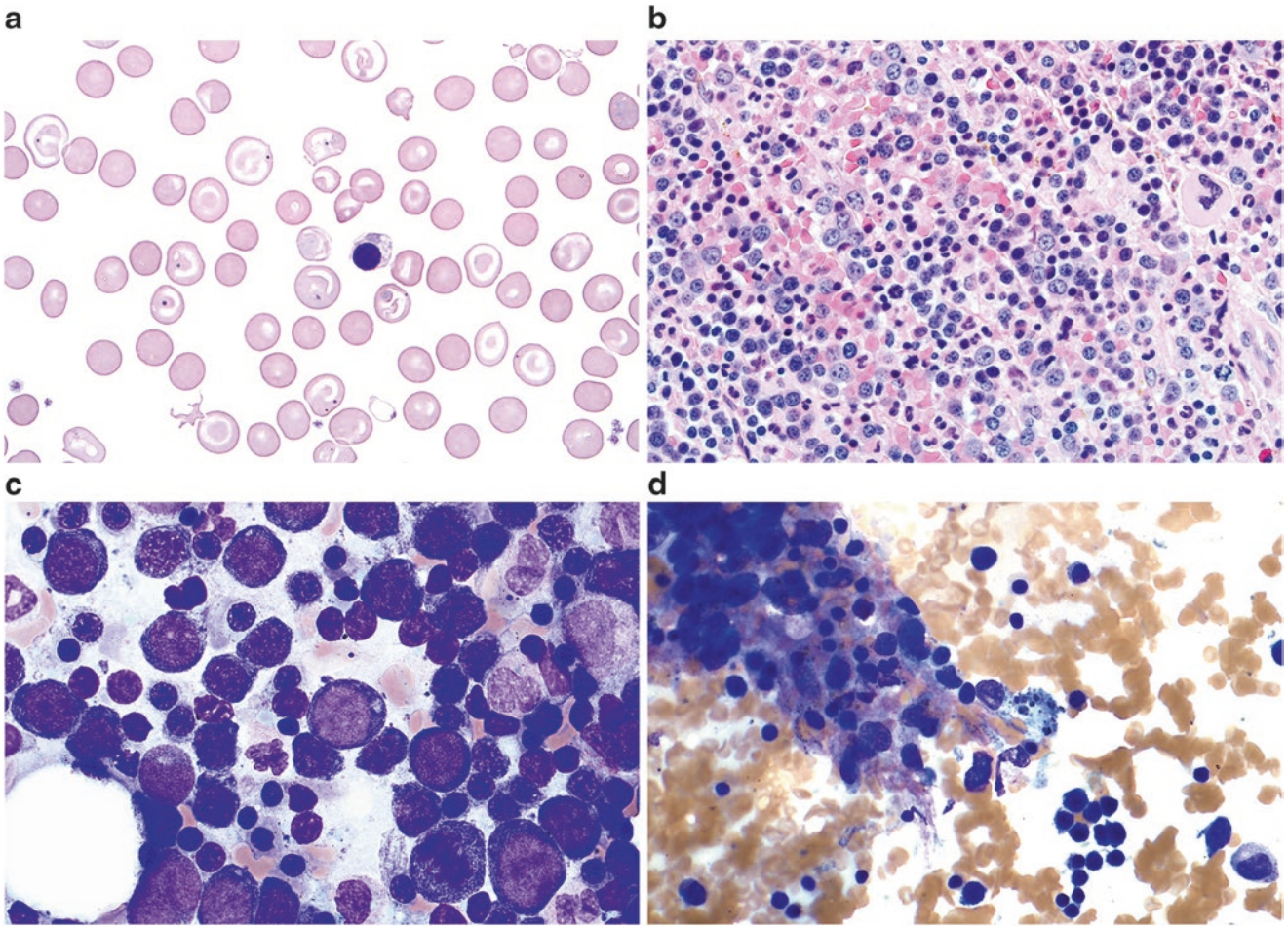

Fig. 4.13 Thalassemia. Thalassemia is an inherited blood disorder resulting from reduced production of hemoglobin. The two most common forms of thalassemia are β-thalassemia and α-thalassemia. (**a**) A peripheral smear from a 27-year-old woman with β-thalassemia intermedia showing severe anemia with nucleated RBCs, microcytes, target cells, and Pappenheimer bodies. (**b**) The bone marrow core biopsy shows a hypercellular marrow with an erythroid hyperplasia. Note the numerous cells with fine chromatin consistent with erythroid pronormoblasts and left-shifted erythropoiesis. (**c**) The aspirate smear confirms the marked erythroid predominance with frequent early erythroid progenitors. (**d**) A bone marrow aspirate smear from a teenage transfusion-dependent β-thalassemia patient shows erythroid hyperplasia and siderophages. Iron overload is a major cause of morbidity in thalassemia

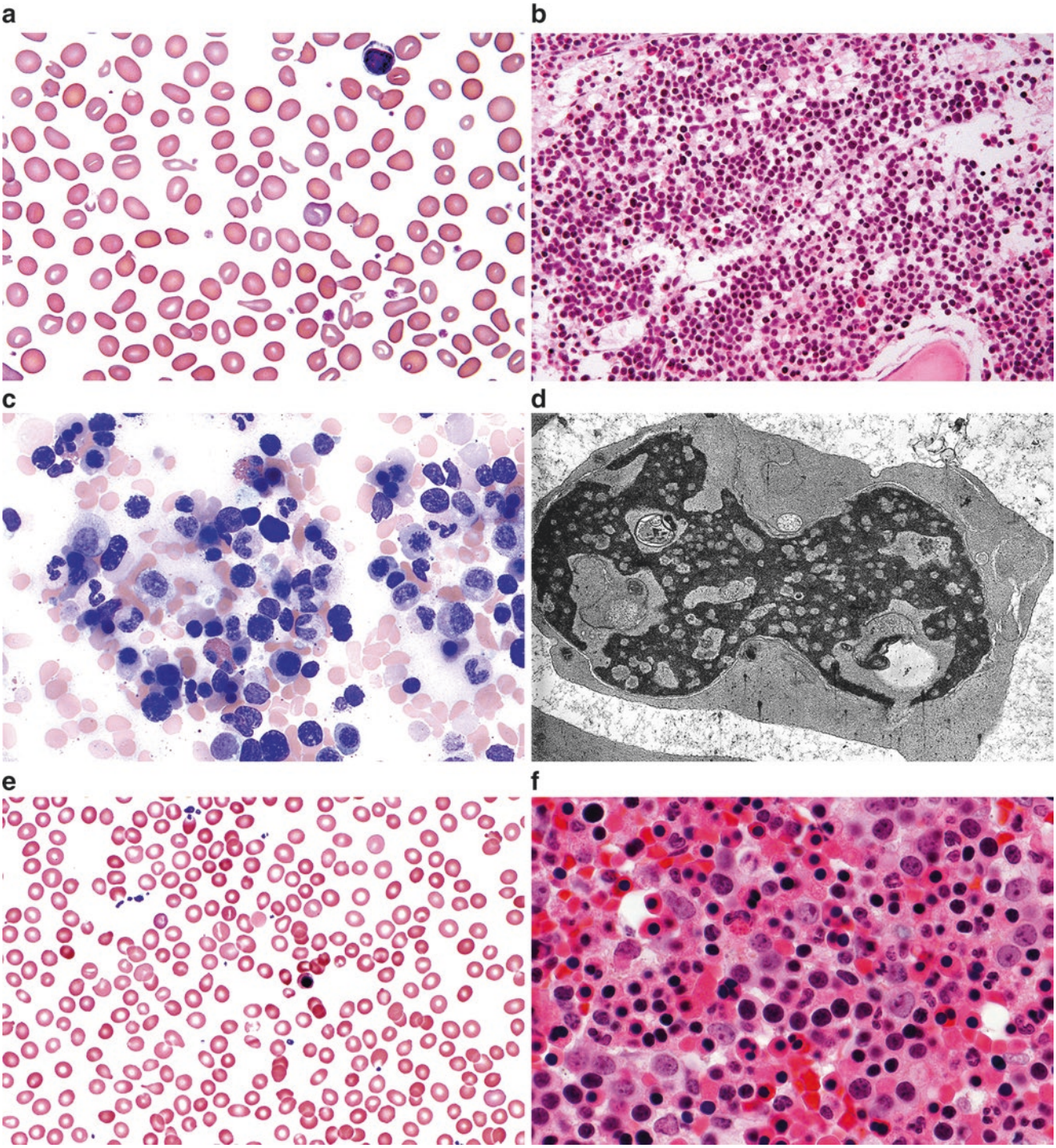

Fig. 4.14 Congenital dyserythropoietic anemia (CDA). (**a**) A peripheral blood smear in CDA type 1, a rare anemia caused by mutations in the *CDAN1* gene located at 15q15.1–15q15.3 and inherited in autosomal recessive fashion, typically shows macrocytic anemia with basophilic stippling. (**b**) As in all types of CDA, a marked erythroid hyperplasia is evident on histology. (**c**) In CDA type 1, the bone marrow aspirate demonstrates megaloblastic erythroid hyperplasia with an increase in binucleate erythroid precursors whose nuclei may partially fuse and be of unequal size. Internuclear chromatin bridges characteristically are seen between polychromatophilic erythroblasts (*not shown*). (**d**) Electron microscopy shows partially fused erythroid precursors with unequal nuclei and characteristic abnormalities of chromatin assembly in the dark-staining areas (heterochromatin) of their nuclei, resulting in a spongy or "Swiss cheese" appearance imparted by electron lucent "holes" (**e**) CDA type 2 is the most common type; it is caused by mutations in *CDAN2* at 20p11.23 and is also autosomal recessively inherited. The peripheral blood smear shows normocytic, normochromic anemia with moderate anisopoikilocytosis and basophilic stippling (*latter not shown*). (**f**) Trephine biopsy section shows an erythroid hyperplasia. Even on histology, binucleated erythroid precursors can be recognized.

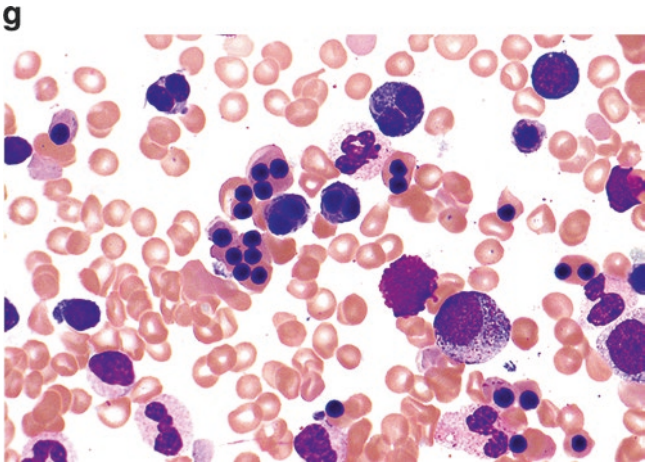

Fig. 4.14 (continued) (**g**) These direct smears from a middle-aged woman with lifelong anemia show a normoblastic erythroid hyperplasia; CDA type 2 is often diagnosed later in life than type 1. Rare early-stage and 10–35% of late-stage erythroid precursors are binucleate; a few are even trinucleate or multinuclear. CDA type 2 is also known as HEMPAS (hereditary erythroblastic multinuclearity with positive acidified serum test). The positive acidified serum lysis test (Ham test), whereby an antigen on CDA-2 red cells combines specifically with about 30% of fresh ABO-compatible normal sera, has been replaced by gel electrophoresis, which can be used to select who should undergo *CDAN2* gene testing, as the band 3 protein on CDA-2 red cells is underglycosylated and migrates faster than normal. CDA type 3 and other types are less common. CDA type 3 has both a familial form (*CDAN3*; autosomal dominant) and a sporadic form. Anemia is mild to moderate and usually macrocytic but sometimes is normocytic. Anisocytosis and poikilocytosis are present, as in CDA types 1 and 2. Like type 1, the bone marrow in CDA type 3 shows megaloblastic erythroid hyperplasia, but the distinguishing feature is the presence of 10–40% "gigantoblasts": large erythroid precursors with a single nucleus or up to 12 nuclei (*not shown*). Interestingly, CDA type 3 patients appear to have an increased risk of lymphoproliferative disorders, although the basis of this risk is unclear

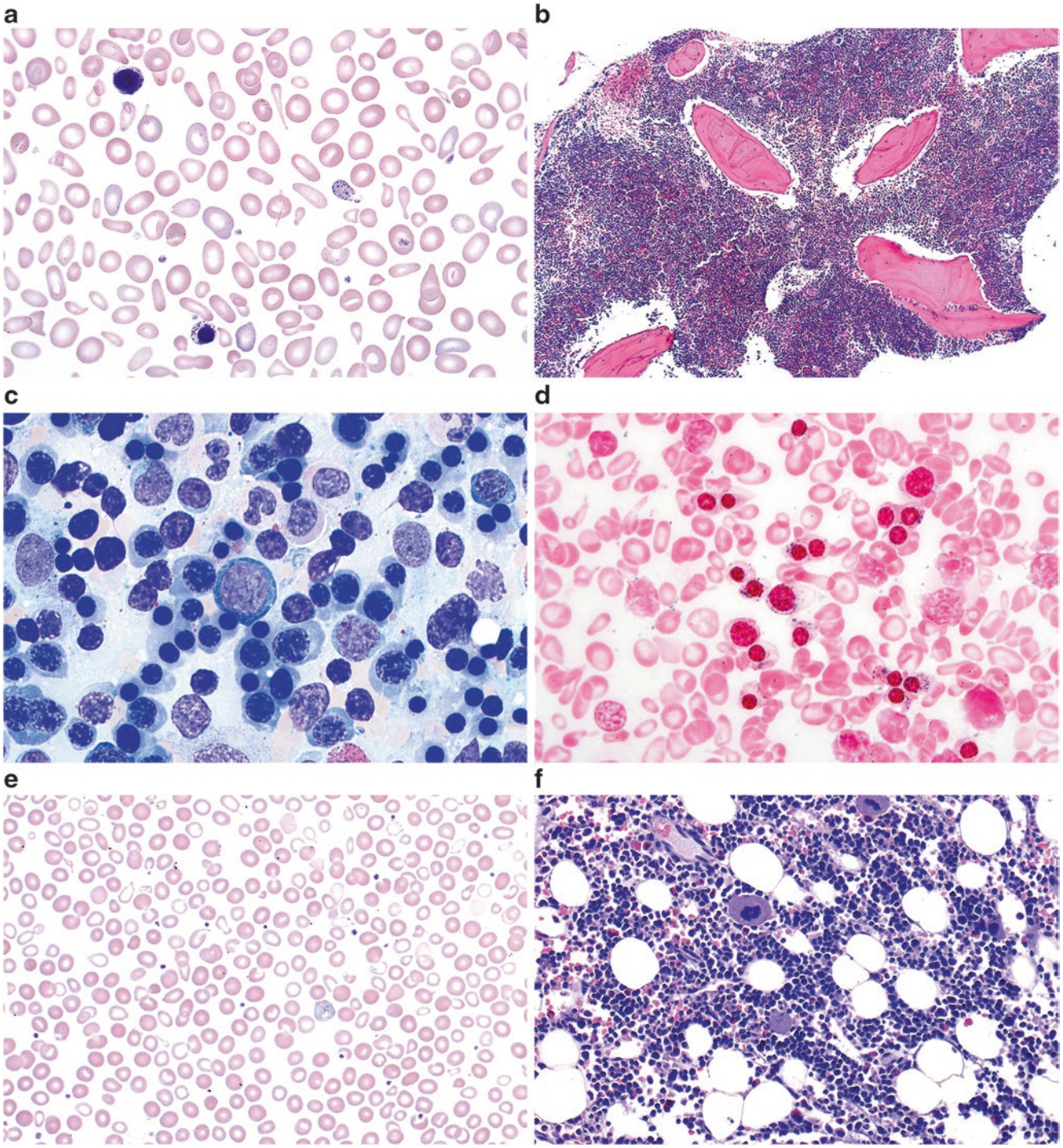

Fig. 4.15 Congenital sideroblastic anemia. (**a**) Peripheral smear from an 8-year-old girl with anemia and fevers, showing marked anisocytosis and poikilocytosis with increased polychromatophilic RBCs, nucleated RBCs, and basophilic stippling. (**b**) The bone marrow biopsy is hypercellular with a marked erythroid hyperplasia. (**c**) The aspirate smear also shows erythroid hyperplasia. (**d**) The iron stain reveals numerous ring sideroblasts. This patient also showed a paucity of B cells with abnormal B-cell maturation by flow cytometric analysis (*not shown*). Germline recessive mutations in *TRNT1* were identified. (**e**) Peripheral smear from a patient with X-linked sideroblastic anemia. The presence of a dimorphic red cell population with rare Pappenheimer bodies is a useful hint at the diagnosis of congenital sideroblastic anemia. (**f**) A bone marrow biopsy showed a hypercellular bone marrow. Although the lymphoid component is increased in this 17-year-old, one should note the predominance of erythroid precursors over granulocytic precursors. Ring sideroblasts were readily identified in the aspirate smears (*not shown*)

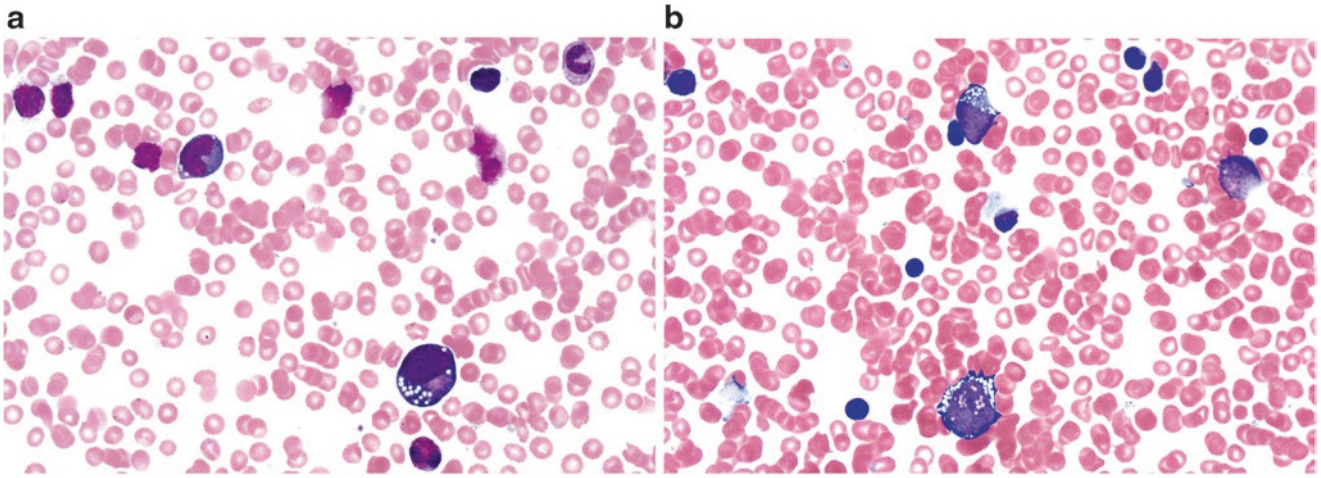

Fig. 4.16 Pearson syndrome. Pearson syndrome is a rare congenital mitochondrial cytopathy typically presenting during infancy. Bone marrow examination reveals vacuoles in both myeloid (**a**) and erythroid (**b**) precursors, with megaloblastic and hyperplastic dyserythropoiesis, including numerous ring sideroblasts (*not shown*) (*Photomicrographs courtesy of* Dr. Teresa Scordino)

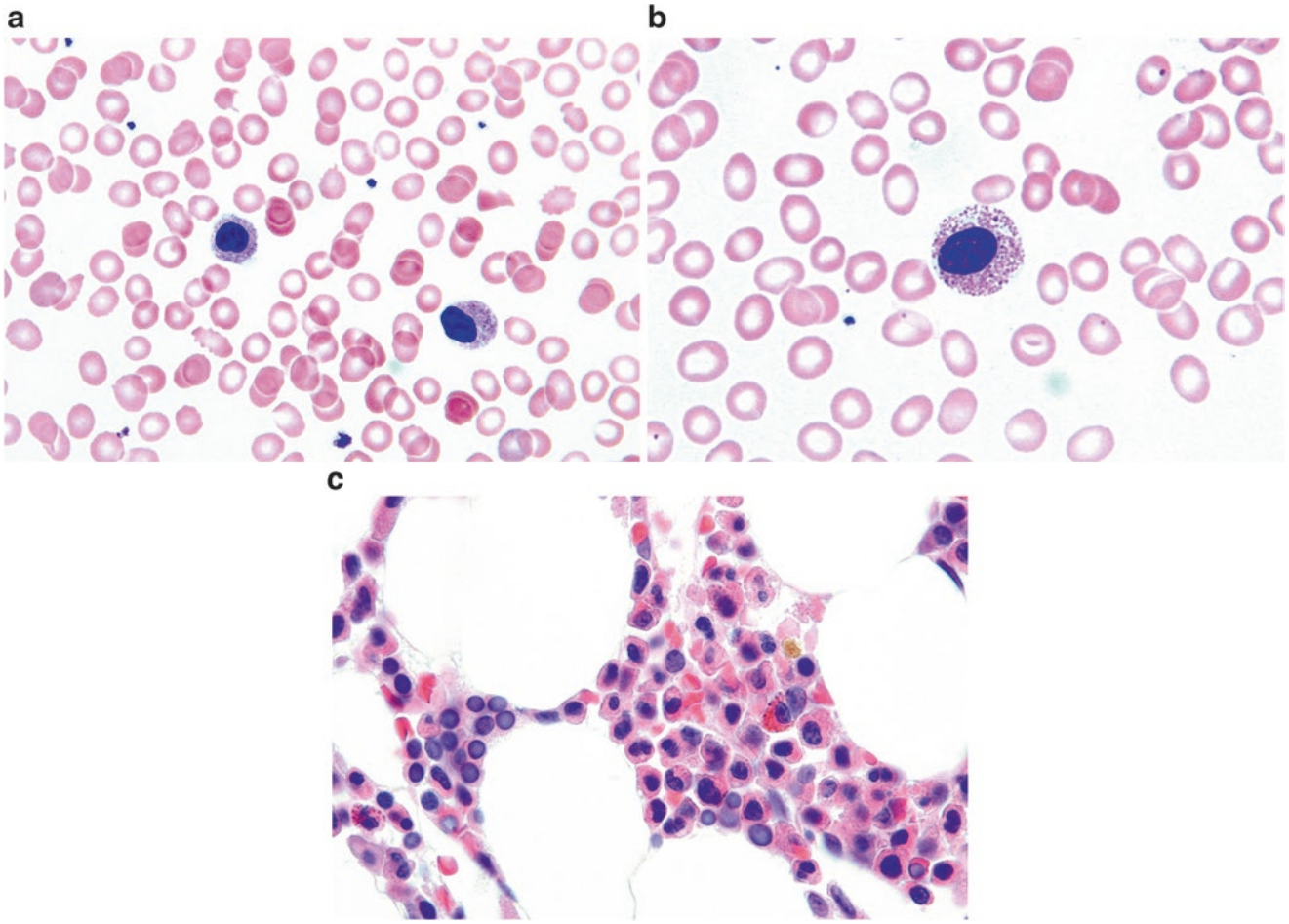

Fig. 4.17 Pelger-Huët anomaly. (**a**) In the Pelger-Huët anomaly, circulating neutrophils have condensed chromatin but hypolobate or monolobate nuclei and can potentially be misinterpreted as immature or dysplastic cells. In the acquired form, or pseudo-Pelger-Huët anomaly, only a subset of neutrophils has this appearance. (**b**) Eosinophils can also display abnormal nuclear segmentation in this disorder. (**c**) Bone marrow core biopsy shows many cells belonging to the neutrophil series, with nuclear lobulation that appears abnormally simple

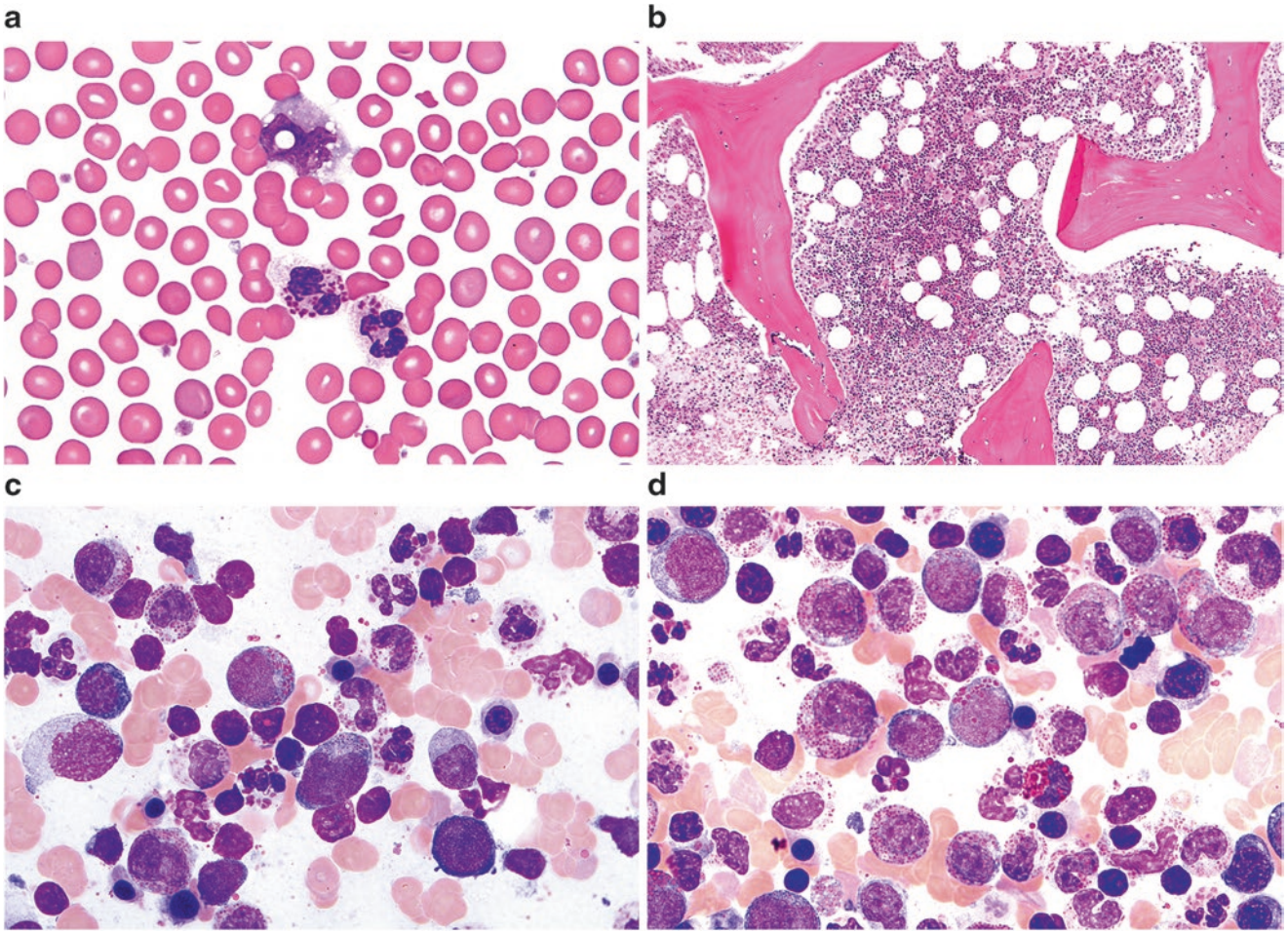

Fig. 4.18 Chédiak-Higashi syndrome. (**a**) This peripheral blood smear from a patient with Chédiak-Higashi syndrome shows the classic finding of giant granules in leukocytes. Although two neutrophils containing these granules are demonstrated here, granules are also seen in eosinophils (and granulocytic precursors), as well as large granular lymphocytes. (**b**) This bone marrow biopsy specimen came from an adolescent male with oculocutaneous albinism and germline autosomal recessive mutations in the *LYST* gene, which encodes a regulator of lysosomal trafficking. The marrow cellularity is normocellular for the patient's age. (**c**) and (**d**) Aspirate smear images show the presence of abnormal large/giant lysosomal granules in the full spectrum of myeloid maturation from blasts to mature neutrophils and eosinophils

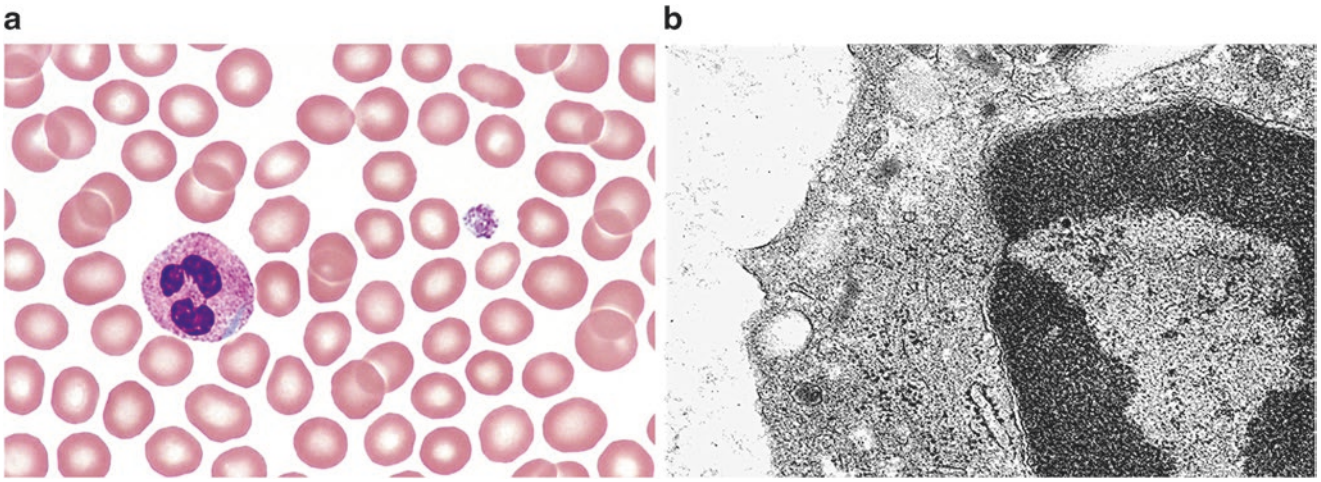

Fig. 4.19 May-Hegglin anomaly. (**a**) This peripheral blood smear is from a teenager with macrothrombocytopenia. Note that the neutrophil contains a basophilic structure that resembles a Döhle body but is larger. (**b**) Ultrastructure of a neutrophil from an infant with "congenital thrombocytopenia" found to have an *MHY9*-related disorder. The typical finding is clusters of randomly distributed ribosomes within highly dispersed filaments in neutrophils. Döhle-like bodies were observed in neutrophils and in occasional eosinophils in the blood (and can also be seen in monocytes and basophils), which also showed moderate thrombocytopenia with giant platelets; bone marrow examination did not contribute much to the diagnosis, aside from showing adequate megakaryocytes

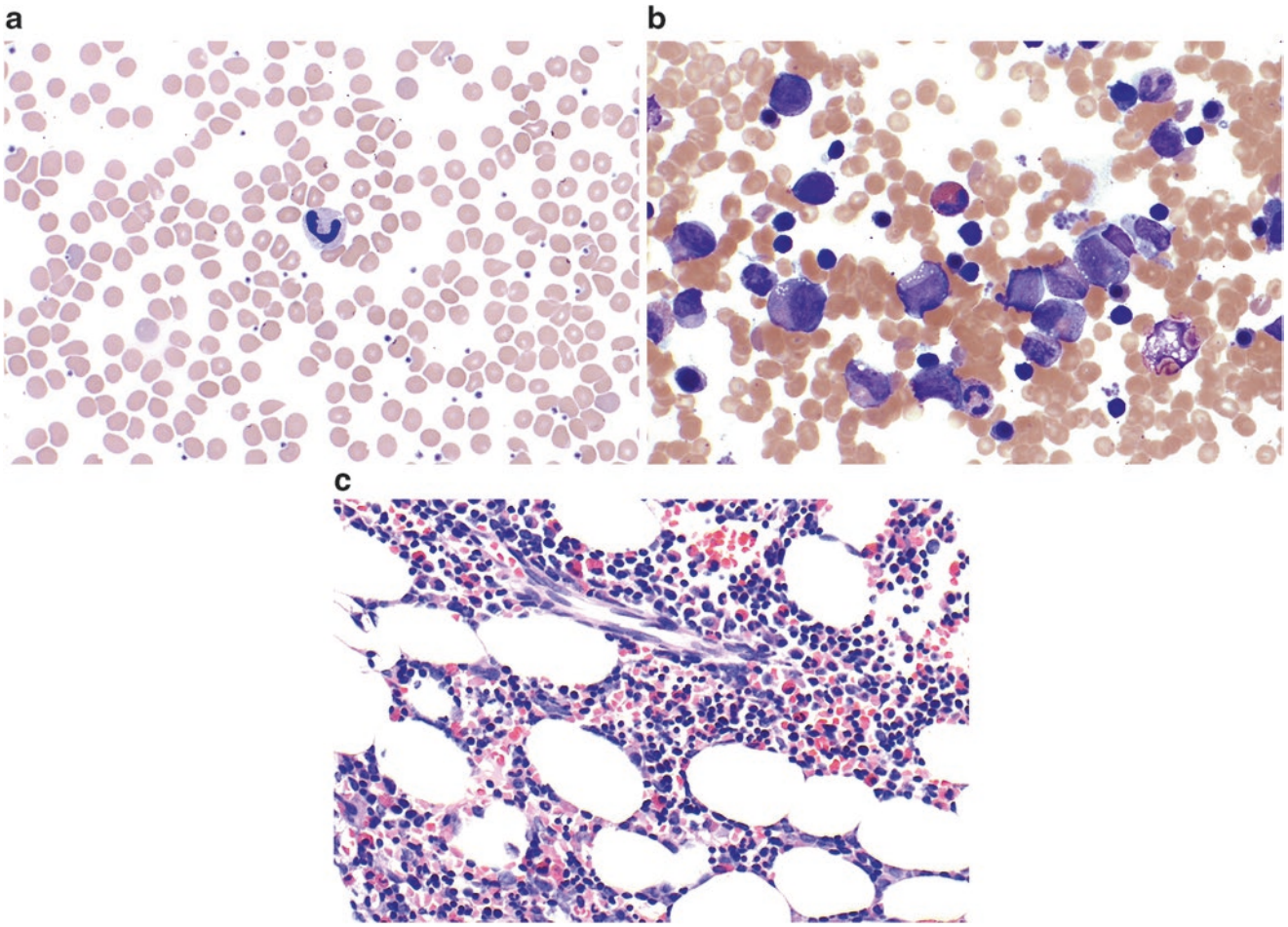

Fig. 4.20 Barth syndrome. Barth syndrome is a cardioskeletal myopathy with neutropenia and abnormal-appearing mitochondria caused by mutations in the *TAZ* gene at Xq28. (**a**) In the peripheral blood smear, vacuoles can be observed in neutrophils. In the original description of Barth syndrome, in addition to vacuoles in about one half of circulating neutrophils, a maturation arrest at the myelocyte stage was observed. (**b**) In this case, the neutrophil series is shifted to immaturity, and both neutrophil precursors and an eosinophil contain cytoplasmic vacuoles. (**c**) As in bone marrow biopsies from many young patients, the core biopsy shows a prominent lymphoid component, but as is characteristic of Barth syndrome, the neutrophil series is left-shifted, with only very rare mature neutrophils

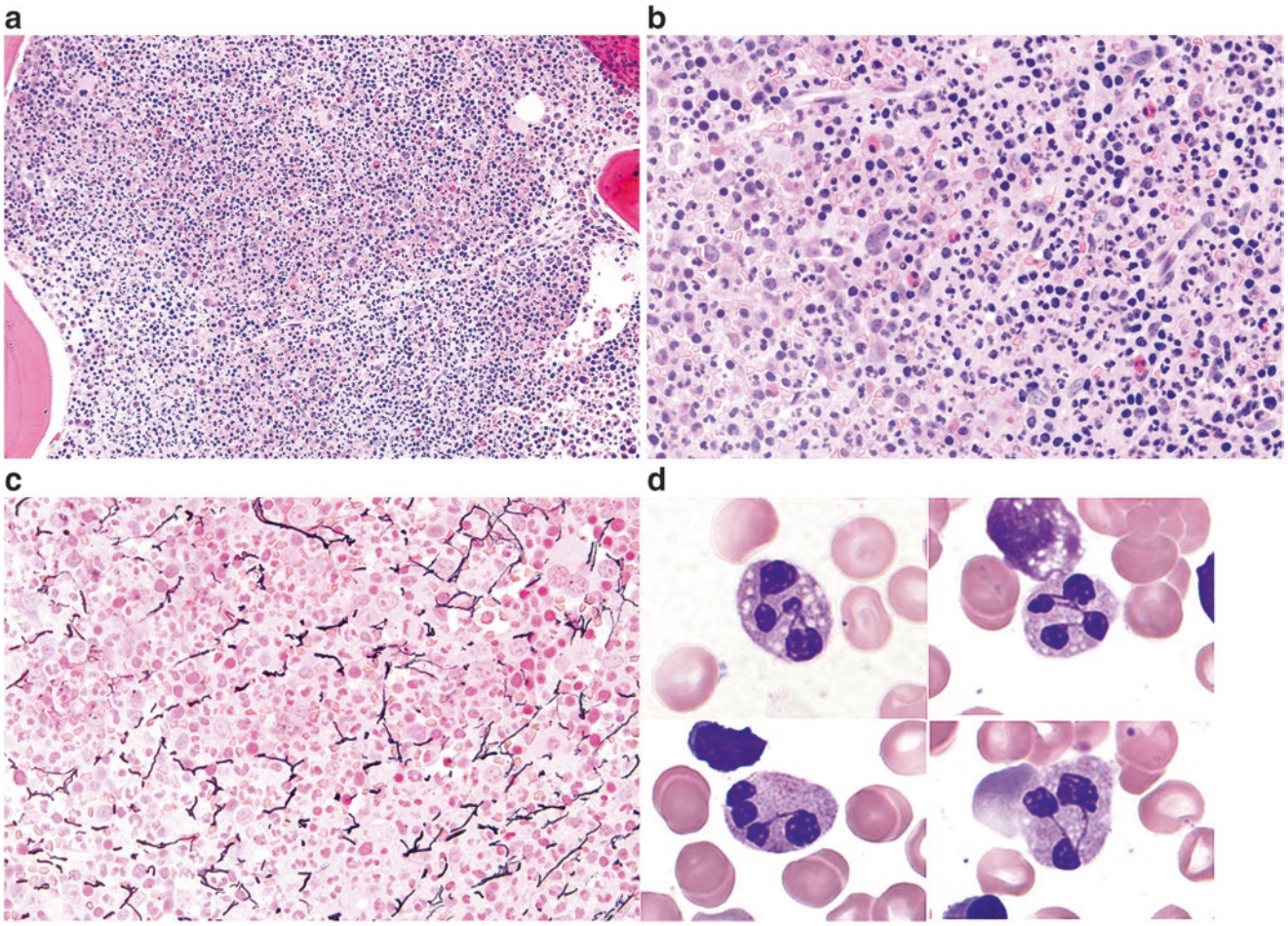

Fig. 4.21 Warts, hypogammaglobulinemia, infections, and myelokathexis (WHIM) syndrome. WHIM syndrome is a congenital immunodeficiency syndrome characterized by germline mutations in *CXCR4*. Patients with WHIM have chronic noncyclic neutropenia. (**a**) Despite the lack of neutrophils in the peripheral blood, the bone marrow is typically hypercellular, with an abundance of maturing myeloid precursors. (**b**) Mature neutrophils are unable to be released from the bone marrow (myelokathexis) and can be seen accumulating and undergoing apoptosis. (**c**) Increased reticulin fibers may be seen on reticulin staining of bone marrow core biopsies in WHIM. (**d**) Aspirate smears demonstrate the presence of unusual neutrophils with condensed nuclear segments connected by thin, wispy strands of chromatin and cytoplasmic vacuoles

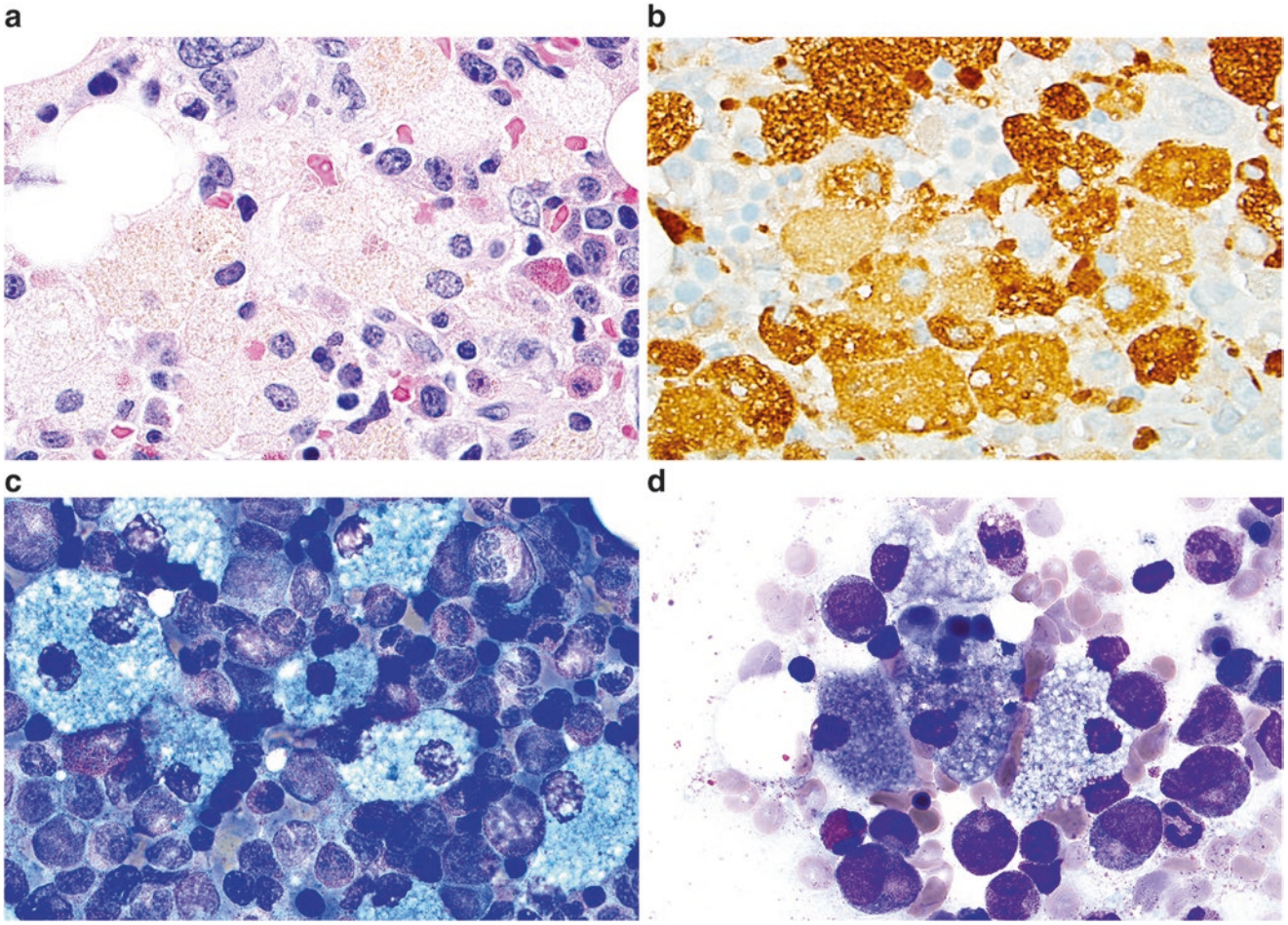

Fig. 4.22 Chronic granulomatous disease (CGD). CGD is an inherited immunodeficiency with germline mutations in genes encoding subunits of the NADPH oxidase complex, such as *CYBA*, *CYBB*, or *NCF1*. Inheritance may be autosomal recessive or X-linked recessive, depending on the gene that is mutated. Despite the presence of granulomas in the lung, skin, lymph nodes, and other tissues, granulomas are not typically seen in bone marrow specimens. However, other distinct features are common in the marrow, including pigmented macrophages (**a**) highlighted by CD68 immunohistochemical stain (**b**). Bone marrow aspirate smears often show the presence of sea-blue histiocytes (**c**) and increased vacuolated histiocytes (**d**), as seen on this marrow specimen from a young male with CGD

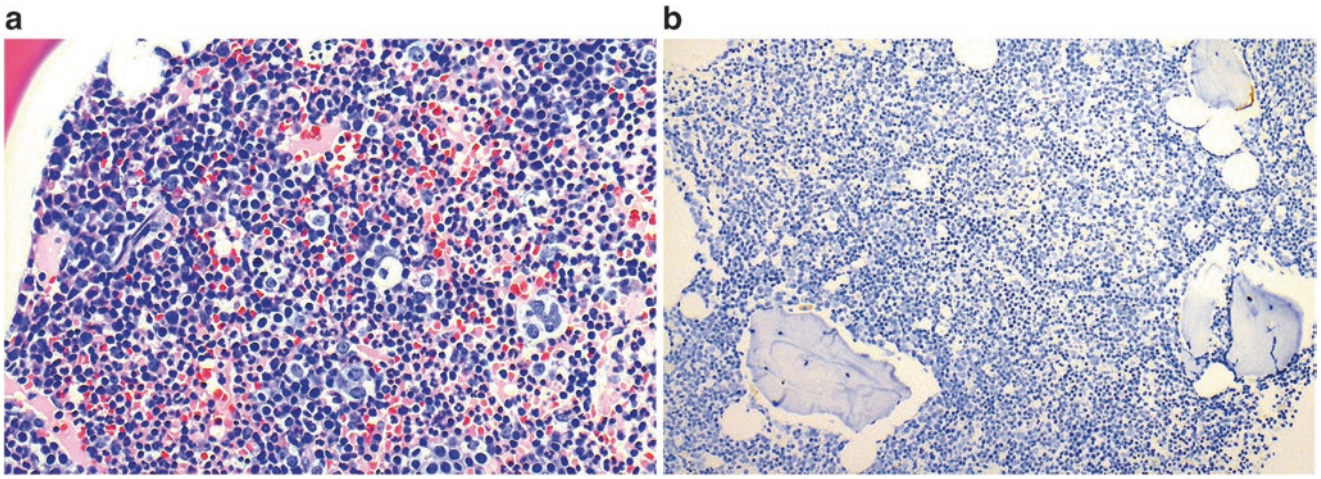

Fig. 4.23 Familial thrombocytopenia with predisposition to AML. This bone marrow comes from a 2-year-old boy with a platelet count of 1×10^9/L, sick contacts, and symptoms of a viral upper respiratory infection, which appeared about 1 week prior to development of bruising. In contrast to the much more common immune/idiopathic thrombocytopenic purpura (ITP), in which megakaryocytes are abundant and present at all stages of maturation, they are nearly absent in this case, with only one present in 17 mm of continuous bone marrow on the H&E-stained section (**a**) and none seen on the CD61 immunostain (**b**). The possibility of viral suppression could not be excluded, so we recommended gene sequencing if the platelet count did not recover, specifically to evaluate for X-linked thrombocytopenia with *GATA1* mutation, congenital amegakaryocytic thrombocytopenia due to *MPL* (thrombopoietin receptor) mutation, familial platelet disorder with associated myeloid malignancy (*RUNX1*), and/or Wiskott-Aldrich syndrome or its attenuated form, X-linked thrombocytopenia (*WAS*). A *germline RUNX1* mutation was found

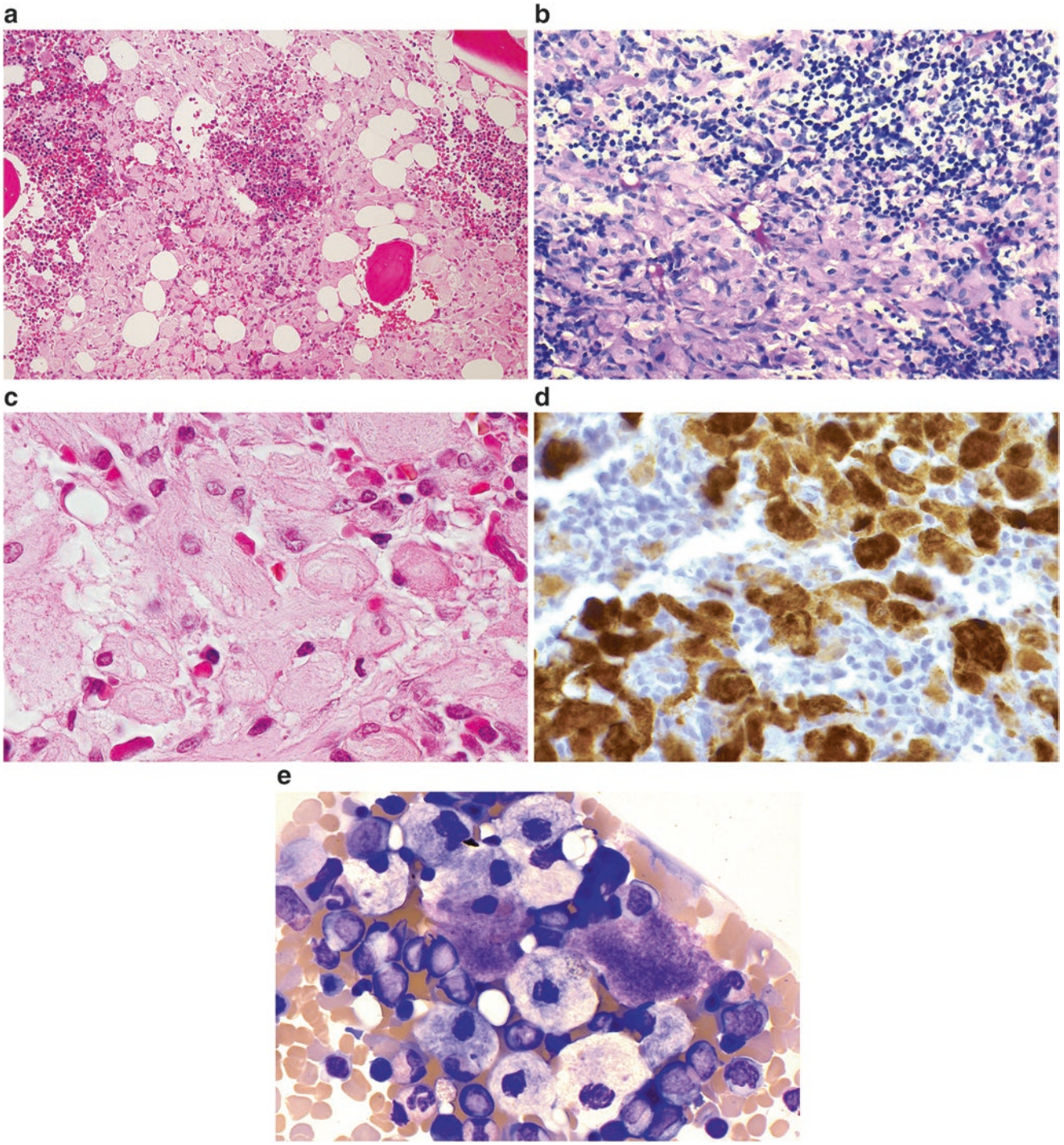

Fig. 4.24 Gaucher disease. (**a**) Bone marrow biopsy from a middle-aged man with thrombocytopenia shows extensive infiltrates of storage histiocytes with eosinophilic cytoplasm. (**b**) The macrophages in Gaucher disease are positive for PAS with and without diastase. (**c**) In this high-power photomicrograph of a core biopsy specimen, one can observe the subtle cytoplasmic striations or fibrillar structures that have caused Gaucher cells to be likened to "wrinkled tissue paper" or "crumpled silk." (**d**) Gaucher cells also stain positively for tartrate-resistant acid phosphatase (TRAP), although the test is now seldom performed. (**e**) Aspirate smear from an Ashkenazi Jewish teenage girl with numerous Gaucher cells demonstrating voluminous pale, basophilic cytoplasm and striations. Gaucher disease can affect people of any ethnic background, but up to 1 in 10 Jews of Eastern European descent are carriers, with a disease prevalence of about 1 in 450 in that population. It should be recognized, however, that pseudo-Gaucher cells can be seen in the bone marrow in a wide variety of other conditions

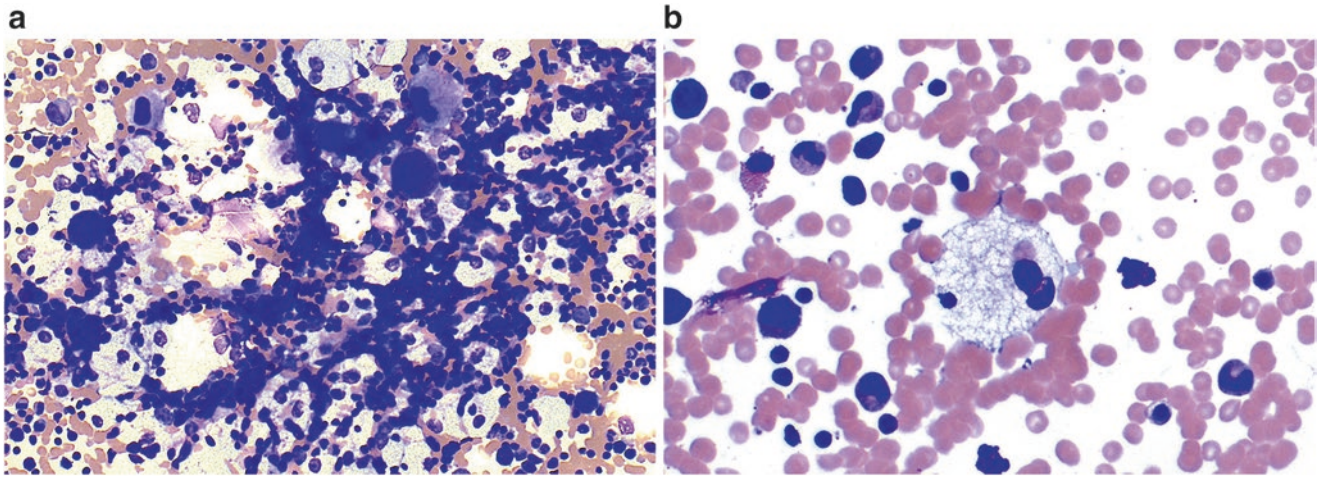

Fig. 4.25 Niemann-Pick disease. (**a**) and (**b**) The macrophages in Niemann-Pick disease have foamy cytoplasm with fine, round lipid-containing vacuoles having a "soap bubble" appearance. Although not depicted here, they are positive for PAS (with and without diastase), Sudan Black B, and oil red O. Similar macrophages can be observed in other storage diseases, such as Tangier disease, hyperlipidemia, fat necrosis, and bone marrow infarction

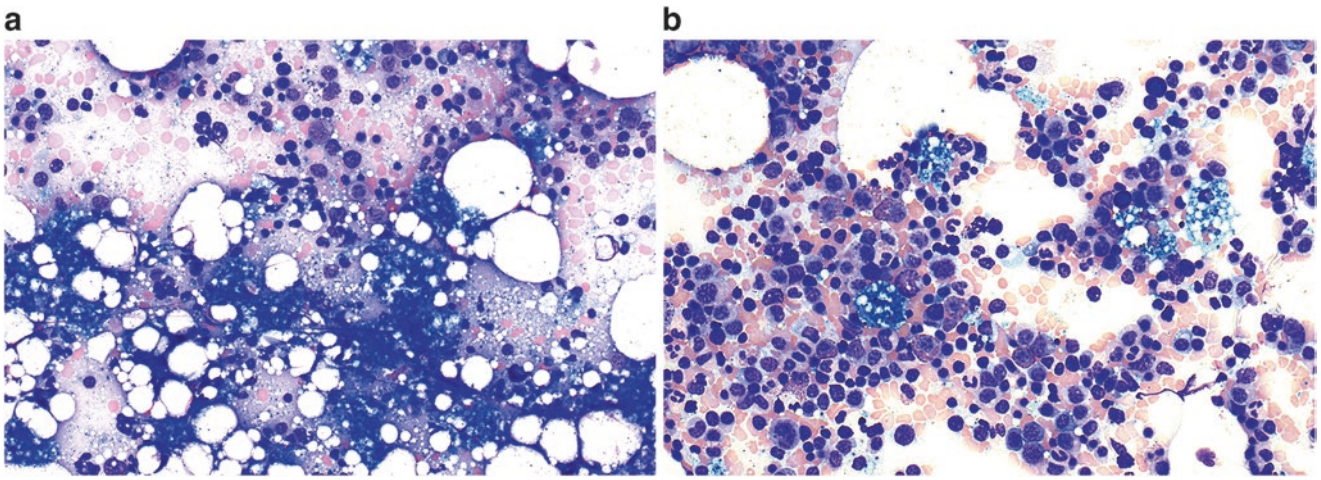

Fig. 4.26 Sea-blue histiocytosis/ceroid lipofuscinosis. (**a** and **b**) Now recognized as a variant of Niemann-Pick disease, the macrophages in sea-blue histiocytosis have coarse, sea-blue, or blue-green granules whose color is attributed to ceroid, which is composed of phospholipids and glycosphingolipids. The granules stain with oil red O and Sudan Black B, and as the pigment ages, it develops a yellow-green autofluorescence, followed by PAS positivity and then acid-fast positivity. But like the other storage diseases mentioned earlier, similar macrophages are seen in other conditions, including those with high cell turnover

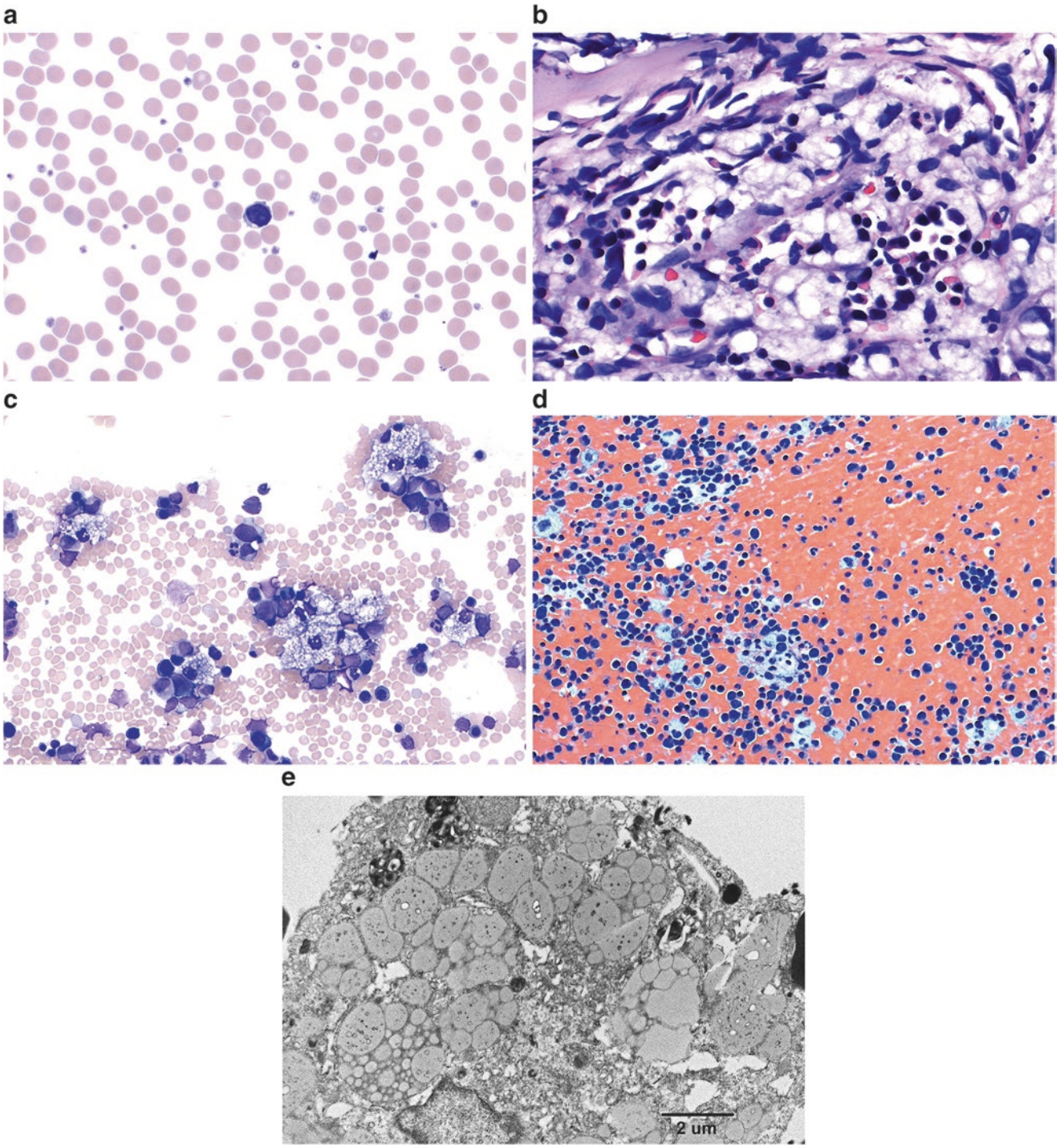

Fig. 4.27 Wolman disease/lysosomal acid lipase deficiency. (**a**) Vacuoles in a peripheral blood lymphocyte from a patient with Wolman disease are shown here. (**b**) High-power photomicrograph of a bone marrow core biopsy in Wolman disease shows an abundance of foamy macrophages. (**c**) Foamy macrophages are found in the bone marrow aspirate of a pediatric Wolman disease patient. Their cholesteryl ester storage content would be reflected by positive staining for oil red O and Cain's Nile blue. This patient had bilateral adrenal calcifications on imaging, a characteristic finding resulting after saponification of fatty acid esters that accumulate in and enlarge the adrenals. (**d**) Foamy macrophages in particle clot are seen in the same patient. (**e**) Electron microscopy shows numerous lipid inclusions

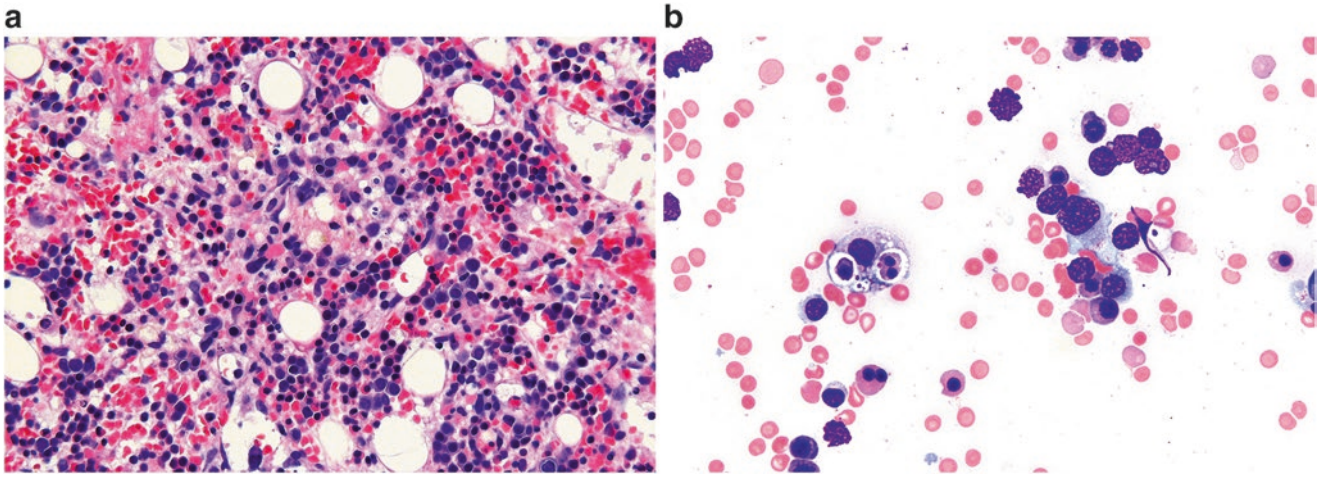

Fig. 4.28 Hemophagocytic lymphohistiocytosis (HLH). Interpretation of hemophagocytosis can be subjective and is neither sensitive nor specific; it is not even required for a diagnosis of HLH, but it was evident in the core biopsy (**a**) and aspirate smears (**b**) of this child with X-linked lymphoproliferative syndrome-1 (XLP1), who succumbed to fulminant EBV infectious mononucleosis. In suspected cases of HLH, bone marrow examination may be sought for treatable underlying causes, including malignancy or infection. Further discussion of HLH can be found in Chap. 14

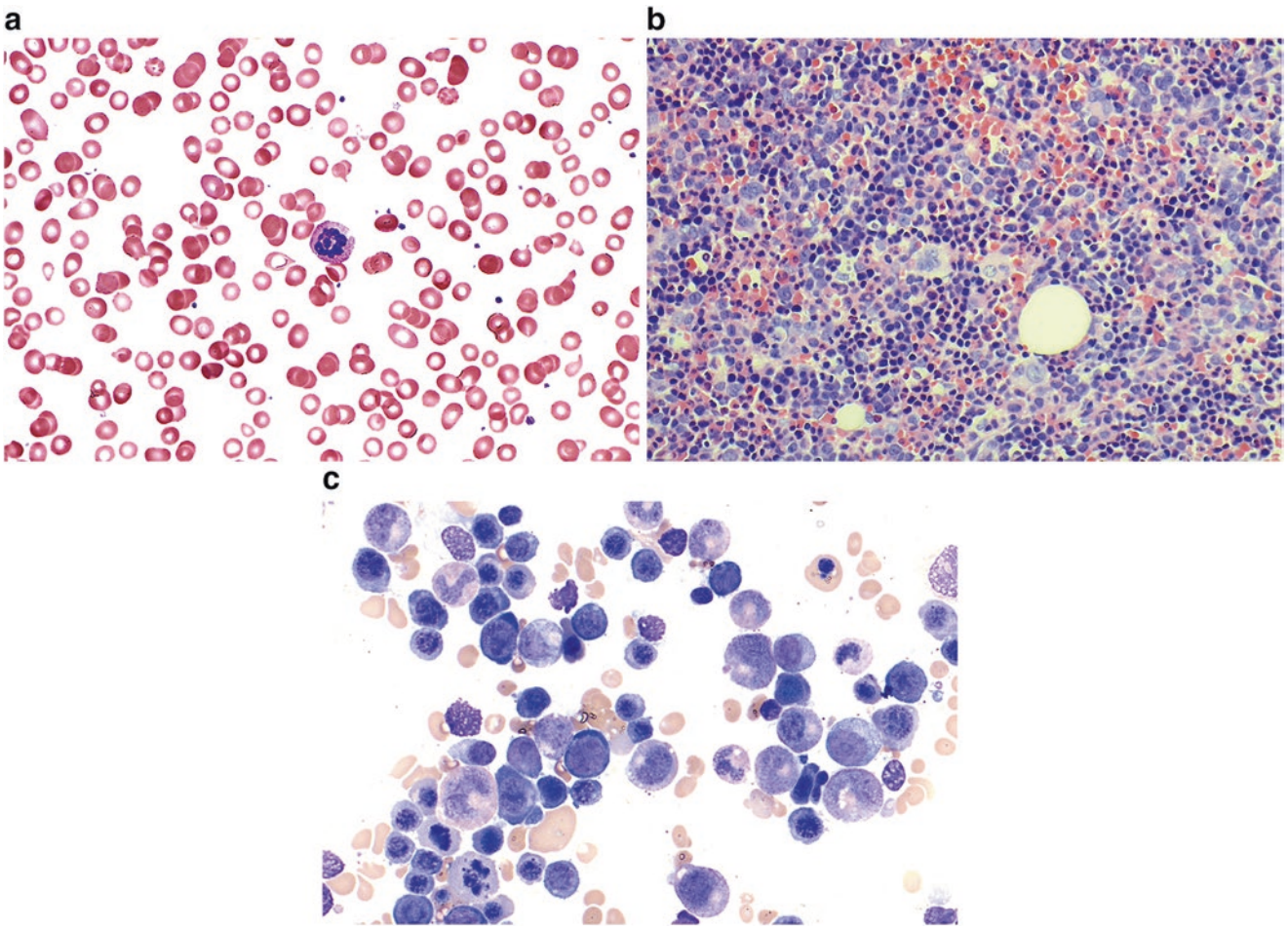

Fig. 4.29 Megaloblastic anemia. (**a**) Peripheral blood smear from a woman with megaloblastic anemia. Note the hypersegmented neutrophil. The second case is an older man who presented with fatigue and dyspnea on exertion, who was found to have hemoglobin of 3.5 g/dL and MCV of 117 fL. Vitamin B12 level was low at <50 pg/mL (normal, 181–914). (**b**) The bone marrow was hypercellular for age (90–95% cellular), with erythroid hyperplasia, megaloblastic maturation and significant dyspoiesis, and readily identifiable giant metamyelocyte and band neutrophils. (**c**)

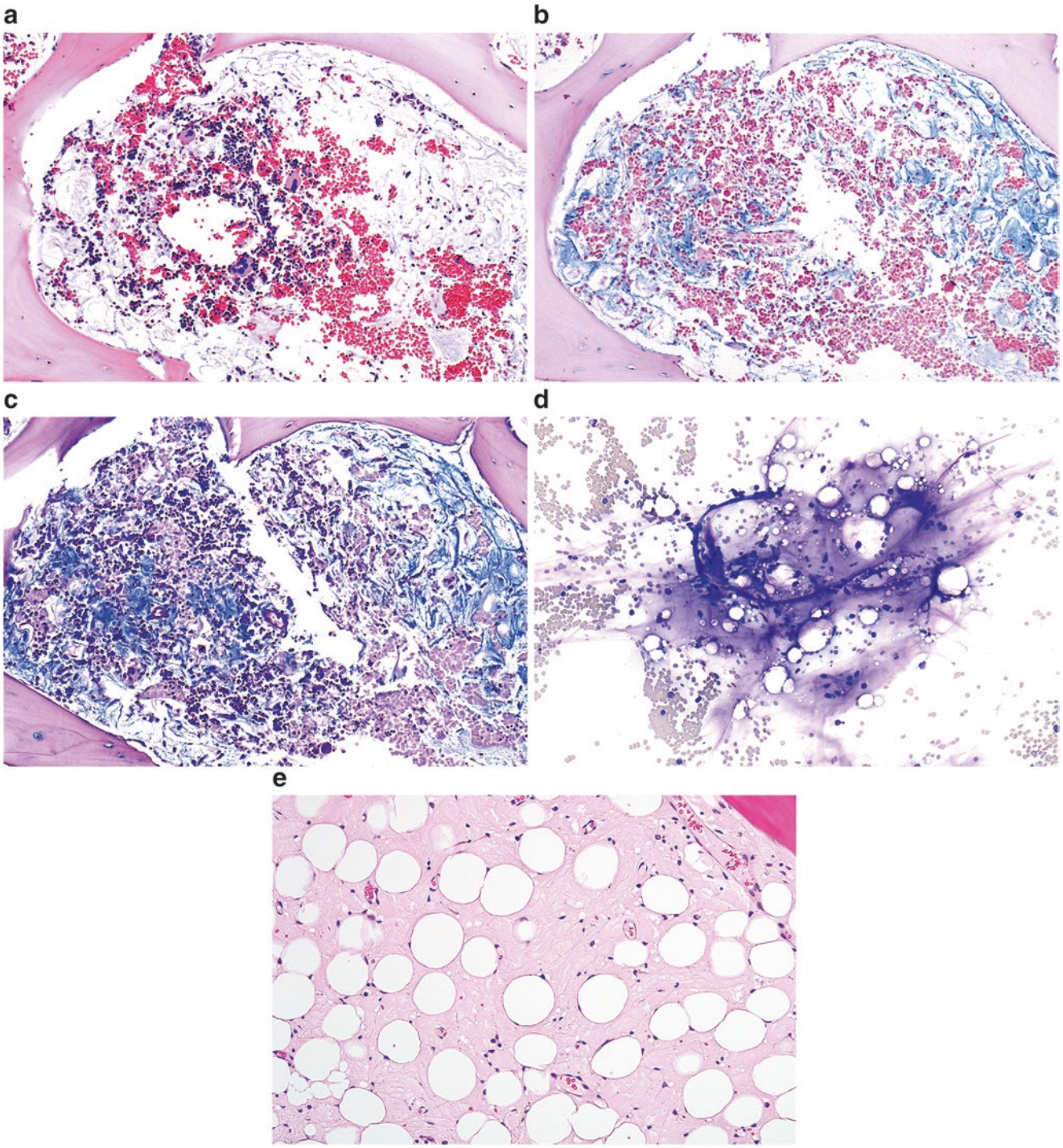

Fig. 4.30 Gelatinous transformation of the marrow/serous fat atrophy. These images come from the bone marrow of a 16-year-old girl with X-linked hypophosphatemic rickets, anorexia nervosa, and rumination syndrome with severe malnutrition. (**a**) The trephine biopsy displays amorphous, bluish, finely granular/fibrillar material with focal atrophy of fat cells and patchy residual hematopoiesis. Alcian blue (pH 2.5) (**b**) and Alcian blue-periodic acid-Schiff (**c**) stains confirm the acid mucosubstance composition of the amorphous material. (**d**) This stromal material shows a blue-pink appearance on Wright-Giemsa stain. Gelatinous transformation/serous fat atrophy is a nonspecific finding associated with anorexia nervosa or cachexia from chronic debilitating illnesses such as infections, malignancy, systemic lupus erythematosus, hypothyroidism, renal or heart failure, celiac disease, intestinal lymphangiectasia, and alcoholism; it also has been seen at sites of irradiation, and it can be seen in patients treated with chemotherapy (**e**). Images of gelatinous transformation are also found in Chap. 2 (Figs. 2.43, 2.44)

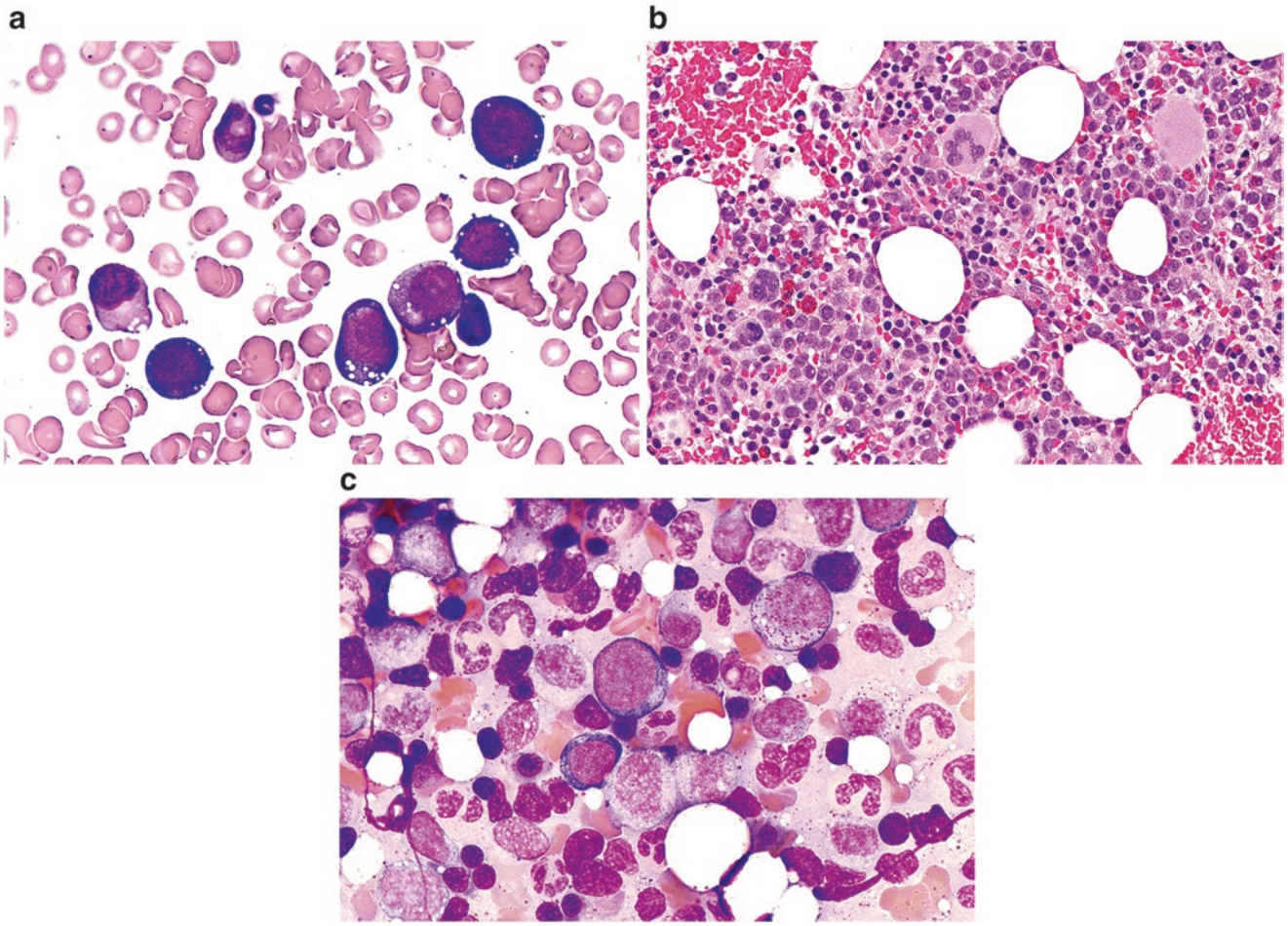

Fig. 4.31 Copper deficiency. Bone marrow aspirate smear (**a**) and core biopsy (**b**) from an elderly man referred to our institution to begin treatment for myelodysplastic syndrome. Vacuoles were seen in both myeloid and erythroid precursors; the serum copper level was found to be very low. The appearance of the bone marrow returned to normal following copper repletion (**c**) (*Images courtesy of* Dr. LoAnn Peterson)

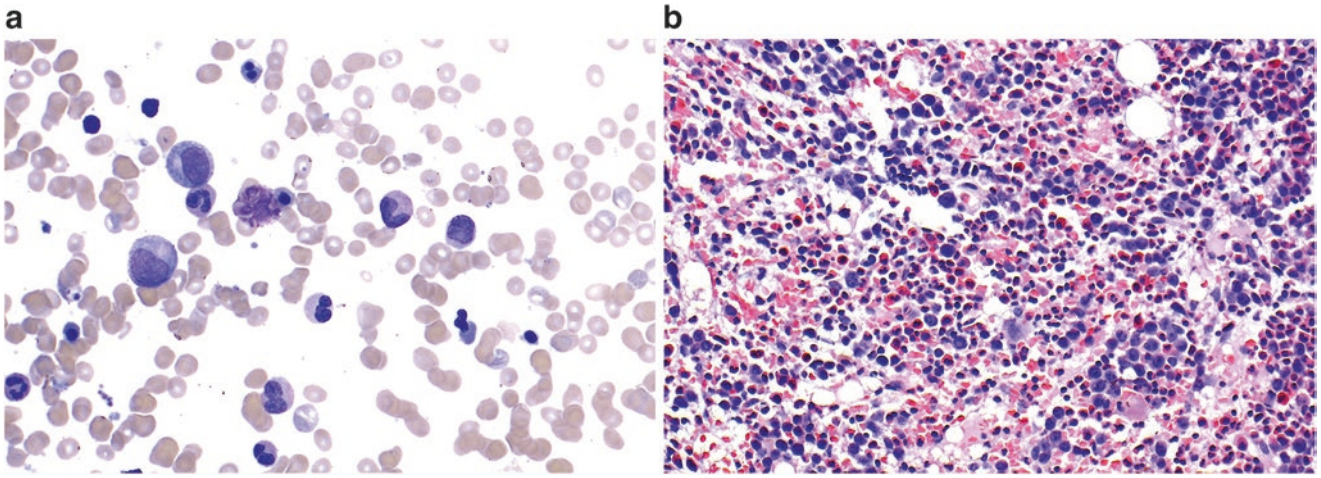

Fig. 4.32 Arsenic toxicity. Arsenic toxicity can result in unilineage or multilineage cytopenias. (**a** and **b**) Bone marrow examination in this case reveals bizarre, megaloblastic dyserythropoiesis with striking karyorrhexis, which can mimic myelodysplastic syndrome or megaloblastic anemia. Arsenic disappears from the blood within a few hours of acute ingestion (the body treats it like phosphate), but because it becomes concentrated by the kidneys, it can be detected for days in the urine. Arsenic has a high affinity for keratin due to high cysteine content, so Mees' lines (transverse white striae) may appear in the fingernails. Hair samples are useful for documenting exposure over the course of several months to a year

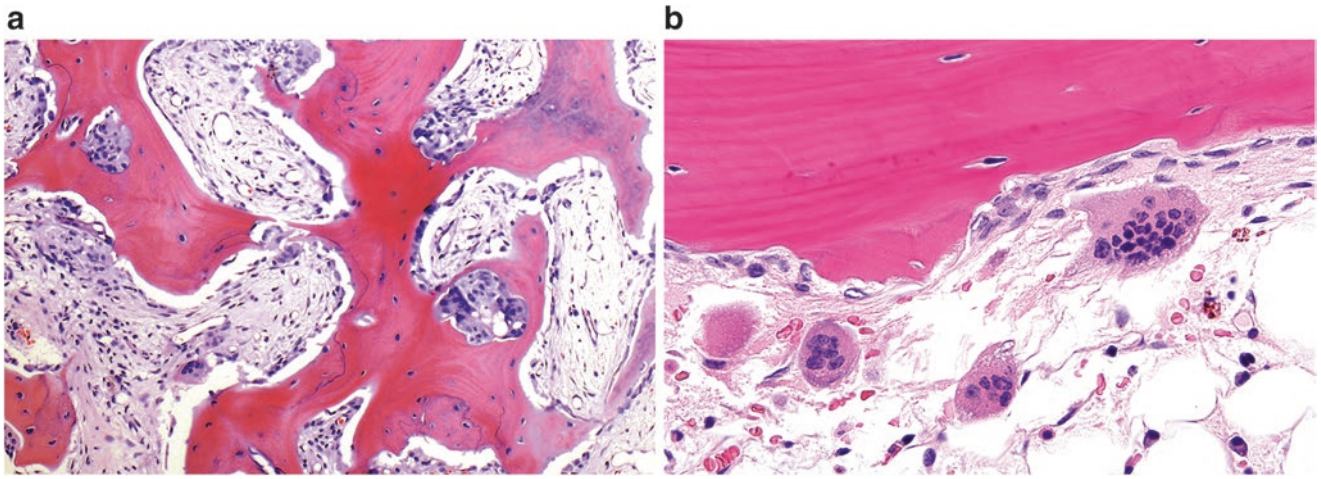

Fig. 4.33 Osteitis fibrosa/renal osteodystrophy. An 87-year-old woman with chronic kidney disease on darbepoetin alfa for several years for associated anemia developed progressive pancytopenia (WBC 1.5 × 10^9/L, hemoglobin 6.2 g/dL with an MCV of 117 fL and scattered dacrocytes, and platelets 30 × 10^9/L) over the course of several months. The bone marrow trephine biopsy (**a**) demonstrated nearly complete replacement by reticulin and collagen fibrosis and markedly thickened, anastomosing bony trabeculae with extensive features of remodeling (scalloped contours, osteoblastic rimming, and osteoclastic resorption, including in depressed resorption bays/Howship's lacunae). The differential diagnosis for such changes is broad and includes myeloid neoplasms (primary myelofibrosis, myelodysplastic syndrome with fibrosis, acute panmyelosis with myelofibrosis, acute megakaryoblastic leukemia), chronic renal failure (renal osteodystrophy) with or without secondary hyperparathyroidism, Paget's disease, systemic mastocytosis, metastatic tumor (carcinoma, classic Hodgkin lymphoma), osteosclerotic myeloma/POEMS syndrome, fracture or previous biopsy site, metabolic disorders, and autoimmune or infectious etiologies. The osteitis fibrosa was attributed to chronic renal disease after an unrevealing workup with normal/negative results of serum and urine protein electrophoresis and immunofixation, flow cytometry immunophenotyping, immunohistochemistry, and conventional cytogenetic analysis to exclude many of the above entities. (**b**) High-power image of osteoblasts and osteoclasts along the bony trabeculae is shown

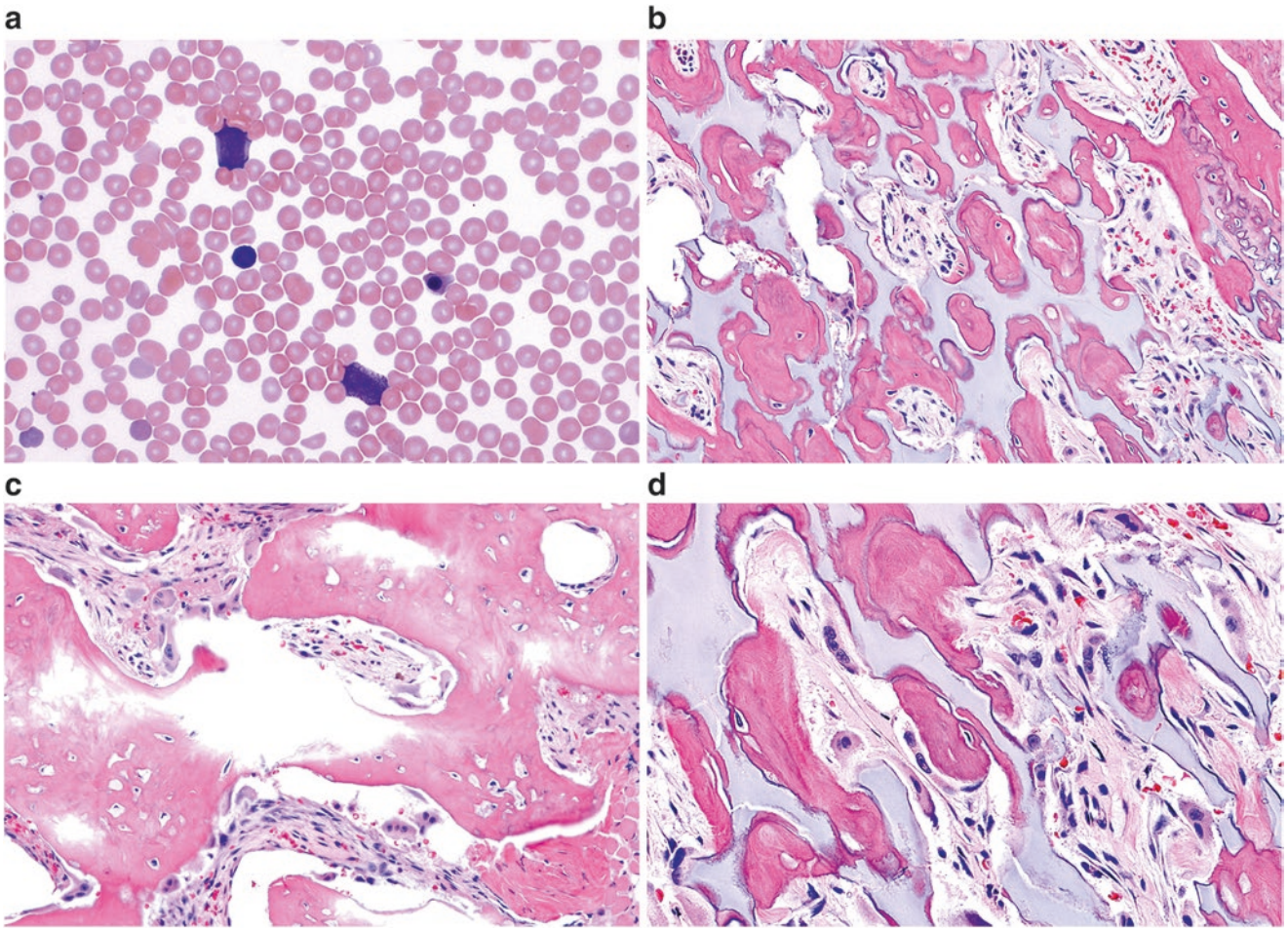

Fig. 4.34 Osteopetrosis. (**a**) Peripheral blood smear from a 10-week-old girl with autosomal recessive osteopetrosis due to two heterozygous pathogenic mutations in the *TCIRG1* gene shows a leukoerythroblastic reaction. Flow cytometry immunophenotyping revealed approximately 10% circulating transitional B cells and 4% myeloid blasts. It makes sense that the blood in osteopetrosis patients can contain elements typically found in the bone marrow, because excessive osteoblastic activity with decreased bone resorption (owing to functionally defective osteoclasts) leads to markedly thickened bone, which together with stromal fibrosis results in obliteration of the marrow space. The rationale for allogeneic hematopoietic stem cell transplantation is that progenitors that can differentiate into functional osteoclasts will promote bone remodeling and a reversal of pancytopenia and extramedullary hematopoiesis (**b**–**d**) Bone marrow biopsy images from a different patient with osteopetrosis illustrate the extent to which hematopoiesis is compromised in osteopetrosis. Note how excessive bone formation leads to obliteration of the marrow space (**b**). Although osteoclasts are abundant in this image of the subcortical marrow (**c** and **d**), they are functionally defective and cannot counterbalance osteoblastic activity (*Images B–D courtesy of* Dr. Tracy George)

Acknowledgment *Work in this chapter was in part supported by the Intramural Research Program of the National Institutes of Health and the NIH Clinical Center.*

Suggested Reading

1. Ansari S, Miri-Aliabad G, Saeed Y. Cystinosis: diagnostic role of bone marrow examination. Turk J Haematol. 2014;31:106.
2. Aprikyan AA, Khuchua Z. Advances in the understanding of Barth syndrome. Br J Haematol. 2013;161:330–8.
3. Bain BJ, Clark DM, Wilkins B. Bone marrow pathology. 4th ed. Wiley-Blackwell: Chichester; 2010.
4. Bakshi NA, Al-Zahrani H. Bone marrow oxalosis. Blood. 2012;120:8.
5. Boutin RD, White LM, Laor T, Spitz DJ, Lopez-Ben RR, Stevens KJ, et al. MRI findings of serous atrophy of bone marrow and associated complications. Eur Radiol. 2015;25:2771–8. https://doi.org/10.1007/s00330-015-3692-5.
6. Busuttil DP, Liu Yin JA. The bone marrow in hereditary cystinosis. Br J Haematol. 2000;111:385.
7. Calvo KR, Vinh DC, Maric I, Wang W, Noel P, Stetler-Stevenson M, et al. Myelodysplasia in autosomal dominant and sporadic monocytopenia immunodeficiency syndrome: diagnostic features and clinical implications. Haematologica. 2011;96:1221–5.
8. Cassinet B, Guardiola P, Chevret S, Schlageter MH, Toubert ME, Rain JD, et al. Constitutive elevation of serum alpha-fetoprotein in Fanconi anemia. Blood. 2000;96:859–63.
9. Colella R, Hollensead SC. Understanding and recognizing the Pelger-Huët anomaly. Am J Clin Pathol. 2012;137:358–66.
10. Cunningham J, Sales M, Pearce A, Howard J, Stallings R, Telford N, et al. Does isochromosome 7q mandate bone marrow transplant in children with Shwachman-Diamond syndrome? Br J Haematol. 2002;119:1062–9.
11. Dhanraj S, Matveev A, Li H, Lauhasurayotin S, Jardine L, Cada M, et al. Biallelic mutations in *DNAJC21* cause Shwachman-Diamond syndrome [letter]. Blood. 2017;129:1557–62.
12. Dror Y, Durie P, Ginzberg H, Herman R, Banerjee A, Champagne M, et al. Clonal evolution in marrows of patients with Shwachman-Diamond syndrome: a prospective 5-year follow-up study. Exp Hematol. 2002;30:659–69.
13. Dulau Florea AE, Braylan RC, Schafernak KT, Williams KW, Daub J, Goyal RK, et al. Abnormal B-cell maturation in the bone marrow of patients with germline mutations in *PIK3CD*. J Allergy Clin Immunol. 2017;139:1032–5.
14. Foucar K, Reichard K, Czuchlewski D. Bone marrow pathology. 3rd ed. Chicago: ASCP Press; 2010.
15. Foucar K, Viswanatha DS, Wilson CS. Non-neoplastic disorders in bone marrow. Washington, DC: American Registry of Pathology in collaboration with the Armed Forces Institute of Pathology; 2008.
16. Ganapathi KA, Townsley DM, Hsu AP, Arthur DC, Zerbe CS, Cuellar-Rodriguez J, et al. GATA2 deficiency-associated bone marrow disorder differs from idiopathic aplastic anemia. Blood. 2015;125:56–70.
17. Gregg XT, Reddy V, Prchal JT. Copper deficiency masquerading as myelodysplastic syndrome. Blood. 2002;100:1493–5.
18. Hoffbrand AV, Pettit JE, Vyas P. Color atlas of clinical hematology. 4th ed. Philadelphia: Mosby/Elsevier; 2010.
19. Hsu AP, Sampaio EP, Khan J, Calvo KR, Lemieux JE, Patel SY, et al. Mutations in GATA2 are associated with the autosomal dominant and sporadic monocytopenia and mycobacterial infection (MonoMAC) syndrome. Blood. 2011;118:2653–5.
20. Ireland RM. Morphology of Wolman cholesterol ester storage disease. Blood. 2017;129:803.
21. Keel SB, Scott A, Sanchez-Bonilla M, Ho PA, Gulsuner S, Pritchard CC, Abkowitz JL, King MC, Walsh T, Shimamura A. Genetic features of myelodysplastic syndrome and aplastic anemia in pediatric and young adult patients. Haematologica. 2016;101:1343–50.
22. Koca E, Buyukasik Y, Cetiner D, Yilmaz R, Sayinalp N, Yasavul U, Uner A. Copper deficiency with increased hematogones mimicking refractory anemia with excess blasts. Leuk Res. 2008;32:495–9.
23. Kuehn HS, Ouyang W, Lo B, Deenick EK, Niemela JE, Avery DT, et al. Immune dysregulation in human subjects with heterozygous germline mutations in CTLA4. Science. 2014;345:1623–7.
24. Lo B, Zhang K, Lu W, Zheng L, Zhang Q, Kanellopoulou C, et al. Patients with LRBA deficiency show CTLA4 loss and immune dysregulation responsive to abatacept therapy. Science. 2015;349:436–40.
25. Maserati E, Pressato B, Valli R, Minelli A, Sainati L, Patitucci F, et al. The route to development of myelodysplastic syndrome/acute myeloid leukemia in Shwachman-Diamond syndrome: the role of ageing, karyotype instability, and acquired chromosome abnormalities. Br J Haematol. 2009;145:190–7.
26. Mellink CH, Alders M, van der Lelie H, Hennekam RH, Kuijpers TW. SBDS mutations and isochromosome 7q in a patient with Shwachman-Diamond syndrome: no predisposition to malignant transformation? Cancer Genet Cytogenet. 2004;154:144–9. https://doi.org/10.1016/j.cancergencyto.2004.02.001.
27. Minelli A, Maserati E, Nicolis E, Zecca M, Sainati L, Longoni D, et al. The isochromosome i(7)(q10) carrying c.258+2t>c mutation of the *SBDS* gene does not promote development of myeloid malignancies in patients with Shwachman syndrome. Leukemia. 2009;23:708–11.
28. Orchard PJ, Fasth AL, Le Rademacher J, He W, Boelens JJ, Horwitz EM, et al. Hematopoietic stem cell transplantation for infantile osteopetrosis. Blood. 2015;126:270–6.
29. Orkin SH, Nathan DG, Ginsburg D, Look AT, Fisher DE, Lux SE. Nathan and Oski's hematology of infancy and childhood. 7th ed. Philadelphia: Saunders/Elsevier; 2009.
30. Pereira I, George TI, Arber DA. Atlas of peripheral blood: the primary diagnostic tool. Philadelphia: Wolters Kluwer Health/Lippincott Williams & Wilkins; 2012.
31. Porta G, Mattarucchi E, Maserati E, Pressato B, Valli R, Morerio C, et al. Monitoring the isochromosome i(7)(q10) in the bone marrow of patients with Shwachman syndrome by real-time quantitative PCR. J Pediatr Hematol Oncol. 2007;29:163–5.
32. Porwit A, McCullough J, Erber WN. Blood and bone marrow pathology. 2nd ed. Churchill Livingstone/Elsevier: Edinburgh; 2011.
33. Pressato B, Marletta C, Montalbano G, Valli R, Maserati E. Improving the definition of the structure of the isochromosome i(7)(q10) in Shwachman-Diamond Syndrome. Br J Haematol. 2010;150:632–3.
34. Pressato B, Valli R, Marletta C, Mare L, Montalbano G, Curto FL, et al. Cytogenetic monitoring in Shwachman-Diamond syndrome: a note on clonal progression and a practical warning. J Pediatr Hematol Oncol. 2015;37:307–10.
35. Preis M, Lowrey CH. Laboratory tests for paroxysmal nocturnal hemoglobinuria. Am J Hematol. 2014;89:339–41.
36. Proytcheva MA. Diagnostic pediatric hematopathology. Cambridge: Cambridge University Press; 2011.
37. Renella R, Wood WG. The congenital dyserythropoietic anemias. Hematol Oncol Clin N Am. 2009;23:283–306.
38. Rezaei N, Aghamohammadi A, Notarangelo LD. Primary immunodeficiency diseases: definition, diagnosis, and management. Berlin: Springer; 2008.

39. Schafernak KT. Gelatinous transformation of the bone marrow from anorexia nervosa. Blood. 2016;127:1374.
40. Spinner MA, Sanchez LA, Hsu AP, Shaw PA, Zerbe CS, Calvo KR, et al. GATA2 deficiency: a protean disorder of hematopoiesis, lymphatics, and immunity. Blood. 2014;123:809–21.
41. Sutton L, Vusirikala M, Chen W. Hematogone hyperplasia in copper deficiency. Am J Clin Pathol. 2009;132:191–9.
42. Townsley DM, Dumitriu B, Young NS. Bone marrow failure and the telomeropathies. Blood. 2014;124:2775–83.
43. Vicari P, Sthel VM. Cystine crystals in bone marrow. N Engl J Med. 2015;373:e27.
44. Wang E, Boswell E, Siddiqi I, CM L, Sebastian S, Rehder C, et al. Pseudo-Pelger-Huët anomaly induced by medications: a clinicopathologic study in comparison with myelodysplastic syndrome-related pseudo-Pelger-Huët anomaly. Am J Clin Pathol. 2011;135:291–303.
45. Weinstein JL, Badawy SM, Bush JW, Schafernak KT. Deconstructing the diagnosis of hemophagocytic lymphohistiocytosis using illustrative cases. J Hematop. 2015;8:113–25.
46. Wickramasinghe SN, Wood WG. Advances in the understanding of the congenital dyserythropoietic anaemias. Br J Haematol. 2005;131:431–6.
47. Xie Y, Pittaluga S, Price S, Raffeld M, Hahn J, Jaffe ES, et al. Bone marrow findings in autoimmune lymphoproliferative syndrome with germline FAS mutation. Haematologica. 2017;102:364–72.